Mathematisches Forschungsinstitut Oberwolfach

Report No. 8/2007

Mini-Workshop: Control of Free Boundaries

Organised by
Charles M. Elliott (Sussex)
Michael Hinze (Hamburg)
Vanessa Styles (Sussex)

February 11th – February 17th, 2007

Abstract. The field of the mathematical and numerical analysis of systems of nonlinear pdes involving interfaces and free boundaries is a burgeoning area of research. Many such systems arise from mathematical models in material science and fluid dynamics such as phase separation in alloys, crystal growth, dynamics of multiphase fluids and epitaxial growth. In applications of these mathematical models, suitable performance indices and appropriate control actions have to be specified. Mathematically this leads to optimization problems with pde constraints including free boundaries. It is now timely to consider such control problems because of the maturity of the field of computational free boundary problems. The aim of the mini-workshop was to bring together leading experts and young researchers from the separate fields of numerical free boundary problems and optimal control in order to establish links and to identify suitable model problems to serve as paradigms for progressing knowledge of optimal control of free boundaries.

Mathematics Subject Classification (2000): MSC: 35-XX, 49-XX, 65-XX IMU: 11, 16, 17.

Introduction by the Organisers

This meeting was attended by 17 participants from Austria, Germany, and Great Britain with expertise from the three areas of optimal control of PDEs, modeling involving free boundary problems and the mathematical and numerical analysis of free boundary problems. Apart from discussing current problems, issues and techniques from the the differing communities the focus of the workshop was set on defining model problems in free boundary control in order to develop the necessary analytical and numerical techniques required to successfully tackle new emerging classes of problems. The governing equations for the dynamics of the interfaces in many of these applications involve surface tension expressed in terms of the mean curvature and a driving force. Here the forcing terms depend on variables

that are solutions of additional pdes which hold either on the interface itself or in the surrounding bulk regions. Examples in the case of solid-liquid interfaces in crystal growth include adjusting the interface to a prescribed shape or ensuring homogeneous doping at the interface. Whereas in the case of epitaxial growth the optimal design would be to ensure a given smoothness of the forming surface. Further examples of control of free boundaries are

- establishing temperature gradients at triple points in Czochralski growth,
- coating with uniform thickness.

The presentations by Emmerich, Griesse, Pinnau, Stinner and Welford concerned modeling and applications for optimal control involving free boundaries. Bänsch, Dziuk and Elliott and Styles gave talks concerning the numerical and mathematical formulations of free boundary problems. Finally, Deckelnick, Garcke, Hintermüller, Hinze, Kunisch and Ziegenbalg focused on the mathematical and numerical analysis of optimal control problems involving free boundaries.

Discussions during the workshop established the following paradigm optimal control problems involving free boundaries:

- *Control of mean curvature flow*
  Here we are concerned with the interface evolution equation

$$V = -H + \theta \tag{1}$$

  where V is the normal velocity of a surface $\Gamma(t)$ whose mean curvature is H. Forced mean curvature flow is considered as a subproblem of curvature driven surfaces occurring in Stefan problems. Also omitting the curvature term leads to control of an eikonal equation. The field variable θ can be used to control the location of the surface. This evolution law as it is posed does not involve field equations off the interface. In certain circumstances the solution can be written as a graph in which case one is controlling a quasi-linear parabolic equation of geometric type. On the other hand it can also be formulated as a level set equation. During the workshop it became clear that each approach to describing the free surface leads to mathematical and numerical issues characteristic to the description of the free boundary.

- *Control of the Hele–Shaw fluid injection problem*
  Denoting by p the pressure in a fluid occupying a two dimensional domain $\Omega(t)$ we have

$$\Delta p = 0 \quad \text{in} \quad \Omega(t) \tag{2}$$

$$V = -p_\nu, \quad p = 0 \quad \text{on} \quad \Gamma(t) \tag{3}$$

  where V is the normal velocity of an advancing front $\Gamma(t)$ separating the wet and dry regions, ν is the normal to $\Gamma(t)$ and the fluid velocity is $-\nabla p$.

The boundary of the fluid region has a fixed portion on which the flux may be prescribed so that

$$p_\nu = Q \quad \text{on} \quad \Gamma_I. \tag{4}$$

This prescribed flux may then be used to control the location of the free boundary and possibly the location of so called weld lines where two portions of fluid meet. Using the transformation, [4],

$$u = \int_0^t p$$

results in an obstacle problem for u in which time t becomes a parameter. There is also the following enthalpy formulation

$$e_t = \Delta p, \quad e \in \mathcal{H}(p) \tag{5}$$

where $\mathcal{H}(\cdot)$ is the Heaviside function.

Thus problem can be used to understand the issues surrounding the optimal control of obstacle problems and degenerate parabolic equations. See [5] for an account of mathematical and numerical approaches to models involving free boundaries being defined by level sets of solutions of variational inequalities and nonlinear degenerate parabolic equations.

During the workshop issues relating to solving obstacle problems by methods such as semi-smooth Newton methods were discussed.

- *Control of convection–driven free surface Stokes flow*

  Control of convection–driven Stokes flow serves as model for control of a more realistic engineering oriented fluid flow problem with a free surface. Denoting by $\boldsymbol{u}, p, T$ the the velocity, pressure, and temperature of the fluid in the domain Ω with a free top surface Γ_f and fixed boundary $\Gamma = \partial\Omega \backslash \Gamma_f$ we have

$$\begin{aligned} -\eta\,\Delta \boldsymbol{u} + \nabla p &= [1 - \beta\,(T - T_{ref})]\,\boldsymbol{g} && \text{in } \Omega \\ \nabla \cdot \boldsymbol{u} &= 0 && \text{in } \Omega \\ -\kappa\,\Delta T + \varrho\,(\boldsymbol{u} \cdot \nabla) T &= 0 && \text{in } \Omega. \end{aligned}$$

  As temperature boundary condition we may take

$$\kappa \frac{\partial}{\partial n} T + \alpha\,(T - T_\infty) = 0 \quad \text{on } \Gamma \cup \Gamma_f,$$

  where T_∞ denotes the environmental temperature. At Γ we impose a no-slip condition

$$\boldsymbol{u} = 0 \quad \text{on } \Gamma.$$

  With the total stress tensor

$$\mathcal{T} = -pI + \eta\left(\nabla \boldsymbol{u} + (\nabla \boldsymbol{u})^\top\right)$$

  we have

$$\begin{aligned} [\boldsymbol{n} \cdot \mathcal{T} \boldsymbol{n}] &= \gamma H \\ [\boldsymbol{t} \cdot \mathcal{T} \boldsymbol{n}] &= 0, \end{aligned}$$

at the free surface, where $[\cdot]$ denotes the jump of a quantity across the free surface, H denotes the mean curvature of the free surface and $\boldsymbol{n}$ and $\boldsymbol{t}$ are surface normal and tangent vectors, respectively. In order to fix the solution, the free surface is required to be normal to the fixed boundary of the container and the volume of fluid is prescribed.

Based on this system of equations one may formulate optimal control problems. The environment temperature T_∞ or additional volume sources in the Stokes or heat equation may serve as control variables. As objectives, one can think of standard tracking-type functionals, involving the fluid velocity and/or the temperature, accounting for flat free surfaces, say. A more general MHD model which contains the model above as a special case is presented in the contribution of Roland Griesse.

Surveys and articles concerning the mathematical and numerical approaches to optimal control of free boundary problems may be found in the conference proceedings [6, 7, 8]. The level set approach to related problems of optimal design are surveyed in [2]. The book [1] contains theoretical results for optimal control of variational inequalities. Also we mention a survey of numerical methods for interface evolution involving curvature, [3]. Finally we remark that many recent references concerning the issues of the workshop are provided at the end of the each extended abstract.

References

[1] V. Barbu *Optimal control of Variational Inequalities* Pitman Research Notes in Mathematics **100** Pitman Boston London Melbourne (1984)

[2] M. Burger and S. Osher *A survey on level set methods for inverse problems and optimal design* Euro. J. Appl. Math. **16** (2005) 263–301

[3] K.P. Deckelnick, G. Dziuk and C.M. Elliott *Computation of Geometric PDEs and Mean Curvature Flow* Acta Numerica (2005) 139–232

[4] C.M. Elliott and V. Janovsky *A variational inequality approach to Hele-Shaw flow with a moving boundary.* Proceedings of the Royal Society of Edinburgh **88A** (1981) 93 -107.

[5] C.M. Elliott and J.R. Ockendon *Weak and variational methods for moving boundary problems.* Pitman Research Notes in Mathematics **59** Pitman Boston London Melbourne 213 pp (1982).

[6] A. Fasano and M. Primicerio (editors) *Free Boundary Problems, Theory Applications* Pitman Research Notes in Mathematics **79** Pitman Boston London Melbourne Pitman, London (1983).

[7] A. Bossavit, A. Damlamian and M. Fremond (editors) *Free Boundary Problems: applications and theory* Pitman Research Notes in Mathematics **121** Pitman Boston London Melbourne Pitman, London (1985)

[8] K.H. Hoffman and J. Sprekels (editors) *Free Boundary Problems, Theory and Applications* Pitman Research Notes in Mathematics **186** Pitman Boston London MelbournePitman, London (1990)

Mini-Workshop: Control of Free Boundaries

Table of Contents

Abstracts

Numerical methods for geometric fourth order problems

Eberhard Bänsch

In the last years, fourth order (and higher) problems arising from geometric evolution laws, such as surface diffusion and Willmore flow, have received much interest. This is partly because they serve as continuum models in materials science suited to describe phenomena on length scales close to the atomistic scale.

This talk is intended to give some insight how to effectively solve these problems computationally.

Optimal control of an eikonal equation

Klaus Deckelnick
(joint work with C.M. Elliott and V. Styles)

Let $I = [-1, 1]$ and suppose that $-1 = \hat{x}_0 < \hat{x}_1 < ... < \hat{x}_{L-1} < \hat{x}_L = 1$ is a partition of I. We are concerned with the following control problem:

(**P**) minimize $J(\underline{a})$, subject to $\underline{a} = (a_1, ..., a_L) \in [\alpha, \beta]^L$,
where

$$J(\underline{a}) = \frac{1}{2} \int_I |y_{\underline{a}}(x, T) - y_T(x)|^2 dx.$$

Here, $0 < \alpha < \beta$ are constants and $y_T \in L^2(I)$ is a given function. Furthermore, $y_{\underline{a}}$ is the solution of the eikonal equation

$$y_t = \sum_{j=1}^{L} a_j \chi_{[\hat{x}_{j-1}, \hat{x}_j)} \sqrt{1 + y_x^2} \quad \text{in } I \times (0, T] \tag{1}$$

$$y(\cdot, 0) = 0 \quad \text{in } I \tag{2}$$

$$y(-1, t) = y(1, t) \quad 0 \le t \le T. \tag{3}$$

Eqn. (1) expresses the fact, that the front $\Gamma(t)$ given by the graph of $y_{\underline{a}}(\cdot, t)$ evolves with normal velocity a_j if $x \in [\hat{x}_{j-1}, \hat{x}_j)$. A similar control problem in which the fronts are described as level sets was recently studied numerically in [3].

Using the methods in [1] it can be shown that (1)–(3) has a unique viscosity solution (in the sense of Ishii [2]) $y = y_{\underline{a}} \in W^{1,\infty}(I \times (0, T))$ which satisfies

$$\|y\|_{W^{1,\infty}(I \times (0,T))} \le C,$$

where C depends on T, $\min\limits_{j=1,...,L} a_j$ and $\max\limits_{j=1,...,L} a_j$. The above bound is the key ingredient when proving that the optimal control problem (P) has a solution $\underline{a}^* \in [\alpha, \beta]^L$. The formal derivation of the adjoint equation leads to a linear transport equation with discontinuous coefficients which seems difficult to analyze. In order

to approximate (P) we therefore discretize (1)–(3) with the help of a Lax–Friedrichs monotone finite difference scheme giving rise to an approximate functional $J_{h,\tau}$, where h and τ are space and time steps respectively. It turns out that at the discrete level, the derivative of $J_{h,\tau}$ can be calculated by means of the adjoint problem. Thus we can use steepest descent in order to compute (local) minima of $J_{h,\tau}$. Fig. 1 shows the result of test calculations for $L = 5$ and $L = 20$ and equally distributed points $\hat{x}_1, ..., \hat{x}_L$. The target function was chosen to be $y_T(x) = 0.5 + \sin(x)$. Besides y_T, the figure shows the discrete solution corresponding to the computed minimum of $J_{h,\tau}$ as well as the values of that minimum.

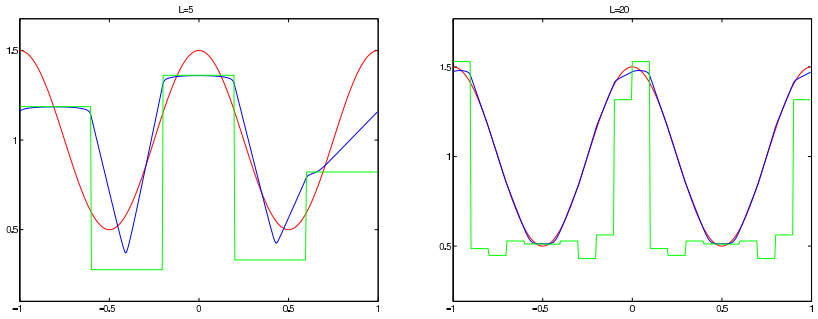

FIGURE 1. L=5 (left) and L=20 (right)

REFERENCES

[1] K. Deckelnick, C.M. Elliott *Propagation of graphs in two–dimensional inhomogeneous media*, Applied Numerical Mathematics **56** (2006), 1163–1178.

[2] H. Ishii, *Hamilton–Jacobi equations with discontinuous Hamiltonians an arbitrary open sets*, Bull. Fac. Sci. Engrg. Chuo. Univ. **28** (1985), 33–77.

[3] S. Leung, J. Qian *An adjoint state method for three–dimensional transmission traveltime tomography using first–arrivals*, Comm. Math. Sci. **4** (2006), 249–266.

Finite Elements on Evolving Surfaces

GERHARD DZIUK
(joint work with Charlie Elliott)

This is a survey of the numerical solution of partial differential equations on evolving surfaces. Such PDEs appear in many applications and it is important to develop numerical methods which are easy to implement and efficient. The discretization depends on the mathematical model for the surface or curve on which the PDE has to be solved. The two main mathematical models are parametric and level set model. In both cases we derive variational forms of a model PDE which then can be used for finite element discretizations. We also discuss numerical analysis.

1. Introduction

There has been burgeoning interest in the computation of partial differential equations on curves and surfaces. Models involving partial differential equations on surfaces arise in many areas including materials science, bio-physics, fluid mechanics and image processing. We mention gradient flows for geometric functionals like Mean Curvature Flow and Willmore-Flow, pattern formation on growing biological organisms, surfactants on the surface of a liquid drop in a flow diffuse and influence its geometric form. In image processing PDEs on surfaces appear in algorithms for segmentation and inpainting on surfaces.

2. PDEs on evolving parametric surfaces

The finite element method is based on the notion of tangential or surface gradient

$$\nabla_\Gamma f = \nabla f - \nabla f \cdot \nu\, \nu$$

of a function which is defined in a neighbourhood of the n–dimensional surface Γ in $\mathbb{R}^{n+1}$ with normal vector ν. Typically we think of $n = 1, 2$. ∇ is the gradient in the ambient space. The tangential gradient only depends on the values of f on the surface. The Laplace-Beltrami operator then is defined as

$$\Delta_\Gamma f = \nabla_\Gamma \cdot \nabla_\Gamma f.$$

As a model problem we take the PDE which models conservation and diffusion of a substance with mass density u on the evolving surface $\Gamma(t)$ for $t \in [0, T]$. For a linear parametrization of the flux one easily derives the equation

$$\dot{u} + u\, \nabla_\Gamma \cdot v - D_0 \Delta_\Gamma u = 0 \tag{1}$$

on the evolving surface Γ with initial value $u(\cdot, 0) = u_0$ on the initial surface $\Gamma(0)$. Here and in the following we assume that Γ has no boundary. For more details concerning the assumptions on $\Gamma(t)$ we refer to [3]. The dot stands for the material derivative

$$\dot{u} = u_t + v \cdot \nabla u$$

with the (vector) velocity v of the surface. Note that this derivative only depends on the values of u on the space-time tube $G_T = \bigcup_{t\in[0,T]} \Gamma(t) \times \{t\}$.

In many publications another form of this PDE is used. That form reveals the influence of the geometric quantities. Decompose the velocity $v = V\nu + T$ into scalar normal velocity V and vector valued tangential velocity T. Then equation (1) can be rewritten as

$$\frac{\partial u}{\partial t} + V \frac{\partial u}{\partial \nu} - uVH + \nabla_\Gamma \cdot (uT) - D_0 \Delta_\Gamma u = 0.$$

In this form of the PDE contains terms like $\frac{\partial u}{\partial \nu}$, which do not only depend on the values of u on the surface. The differential equation contains the mean curvature, which consists of second derivatives "of Γ" and it needs the velocity of the surface explicitly.

A variational form of (1) is given by

$$\frac{d}{dt}\int_\Gamma u\varphi + \int_\Gamma D_0 \nabla_\Gamma u \cdot \nabla_\Gamma \varphi = \int_\Gamma u\dot{\varphi} \quad \forall \varphi \tag{2}$$

for any suitable test function φ. This form of the PDE is the basis for a finite element discretization. The smooth surface $\Gamma(t)$ is approximated by a polyhedral surface $\Gamma_h(t)$. It consists of triangles (simplices) T_h in space,

$$\Gamma_h(t) = \bigcup_{T_h \in \mathcal{T}_h(t)} T_h,$$

which form an admissible triangulation. The vertices $a_j(t) \in \Gamma(t)$, $(j = 1, \ldots, N)$ of the triangles are taken to sit on the smooth surface. We use piecewise linear finite elements on the discrete surface,

$$S_h(t) = \{\eta \in C^0(\Gamma_h(t)) |\, \eta|_{T_h} \in \mathbb{P}_1(T_h), T_h \in \mathcal{T}_h(t)\},$$

and we use a moving nodal basis: $\varphi_j(\cdot, t) \in S_h(t), \varphi_j(a_i(t), t) = \delta_{ij}$. Consequently the material derivative of a basis function φ_j with respect to the discrete surface vanishes:

$$\dot{\varphi}_j = \frac{\partial \varphi_j}{\partial t} + v_h \cdot \nabla \varphi_j = 0.$$

Here the velocity of the discrete surface $\Gamma_h(t)$ is defined as the interpolant $v_h(x, t) = \sum_{j=1}^N V_j(t)\varphi_j(x, t)$ with $V_j(t) = v(a_j(t), t) = \frac{d}{dt}a_j(t)$ being the velocity of the nodes of the discrete surface.

The spatially discrete scheme for the solution of (1) now is to compute $u_h(\cdot, t) \in S_h(t)$, such that with $u_{h0} \in S_h(0)$ one has $u_h(\cdot, 0) = u_{h0}$ on $\Gamma_h(0)$ and

$$\frac{d}{dt}\int_{\Gamma_h} u_h\varphi + \int_{\Gamma_h} D_0 \nabla_{\Gamma_h} u_h \cdot \nabla_{\Gamma_h} \varphi = \int_{\Gamma_h} u_h\dot{\varphi} \tag{3}$$

for all discrete test functions $\varphi \in S_h(t)$.

If we now write the matrix-vector form of this ODE system with the evolving mass matrix M and stiffness matrix S,

$$M(t)_{ij} = \int_{\Gamma_h(t)} \varphi_i\varphi_j, \; S(t)_{ij} = \int_{\Gamma_h(t)} D_0 \nabla_{\Gamma_h}\varphi_i \cdot \nabla_{\Gamma_h}\varphi_j$$

and the vector $u(t) = (u_1(t), \ldots, u_N(t))$ of the coefficients of $u_h = \sum_{j=1}^N u_j\varphi_j$, then the following little Lemma holds true.

Lemma 1. *The ODE system*

$$\frac{d}{dt}\left(M(t)u\right) + S(t)u = 0 \tag{4}$$

is equivalent to the spatially discrete system (3).

Note that in contrast to the form (2) of the PDE our spatially discrete form (4) does not contain the mean curvature of the evolving surface and does not need the computation of the velocity but only the actual position of the evolving surface. Under suitable assumptions on the continuous surface and on the continuous solution we proved the following error estimates. By the lift u_h^l of the discrete solution

we understand $u_h^l(a(x,t),t) = u_h(x,t)$ for the orthogonal projection $a(x,t) \in \Gamma(t)$ of the point $x \in \Gamma_h(t)$.

Theorem 1. *Let u be the continuous solution on Γ and u_h the discrete solution on Γ_h. With the lift u_h^l of u_h one has the error estimate*

$$\sup_{t\in(0,T)} \|u(\cdot,t) - u_h^l(\cdot,t)\|^2_{L^2(\Gamma(t))} + \int_0^T \|\nabla_\Gamma(u(\cdot,t) - u_h^l(\cdot,t))\|^2_{L^2(\Gamma(t))} dt \le ch^2$$

with some constant c which depends on norms of the continuous solution. Here h is the maximal grid size on the discrete surface.

For detailed assumptions and dependencies and for test computations and numerical results see [3].

This method, which we call "Evolving Surface Finite Element Method" (ESFEM), is a generalization to the instationary case of a finite element method for stationary equations on stationary surfaces. That finite element method for the Laplace-Beltrami operator was introduced in [2].

The method presented here is applicable to more general problems and to highly nonlinear equations. Examples for parabolic problems on stationary surfaces can be found in [4].

3. PDEs on implicit surfaces

Let now Ω be a bounded open subset of $\mathbb{R}^{n+1}$ and assume that the surface on which we want to solve the PDE is given as the zero level set of a sufficiently smooth scalar function ϕ,

$$\Gamma(t) = \{x \in \Omega : \phi(x,t) = 0\},$$

where we assume that $\nabla\phi(\cdot,t) \neq 0$ in Ω.
The geometric quantities now are given by

$$\nu = \frac{\nabla\phi}{|\nabla\phi|}, \quad H = -\nabla\cdot\nu, \quad P = I - \nu\times\nu.$$

The Eulerian tangential gradient on the levels of ϕ is defined as

$$\nabla_\phi f = \nabla f - \nabla f\cdot\nu\,\nu = P\nabla f$$

and the Eulerian Laplace-Beltrami-Operator

$$\Delta_\phi f = \nabla_\phi \cdot \nabla_\phi f.$$

Similarly as for the parametric approach in the previous section we now derive a level set version of (1) in variational form. We assume that the level sets of ϕ move with a given velocity $v = v(x,t)$, $x \in \Omega$, $t > 0$.

$$\frac{d}{dt}\int_\Omega u\eta|\nabla\phi| + \int_\Omega D_0\nabla_\phi u\cdot\nabla_\phi\eta|\nabla\phi| = \int_\Omega u\dot\eta\,|\nabla\phi| \tag{5}$$

for any test function η. Now, $\dot\eta = \eta_t + v\cdot\nabla\eta$. Obviously we have imposed natural Neumann-type boundary conditions. We also have assumed that the boundary of the domain Ω is a level set of the function ϕ.

The co-area formula and some geometric analysis then guarantee, that (5) implies the PDE (1) on Γ for smooth ϕ and u.

For more detailed discussions of the method and for clear assumptions on the data we refer to [5] and [6].

We discretize the variational form (5) on a fixed time-independent grid on Ω by piecewise linear finite elements. The implementation then is quite straightforward.

For elliptic problems on stationary level sets such a finite element method was introduced in [1].

References

[1] M. Burger *Finite element approximation of elliptic partial differential equations on implicit surfaces*, CAM-Report 05-46 UCLA (2005).

[2] G. Dziuk *Finite elements for the Beltrami operator on arbitrary surfaces*, in: S. Hildebrandt, R. Leis (eds.): Partial differential equations and calculus of variations. Lecture Notes in Mathematics Springer Berlin Heidelberg New York London Paris Tokyo **1357** (1988) 142–155.

[3] G. Dziuk, C. M. Elliott *Finite elements on evolving surfaces*, IMA Journal of Numerical Analysis **27** (2007), 262–292.

[4] G. Dziuk, C. M. Elliott, *Surface finite elements for parabolic equations*, to appear in Journal of Computational Mathematics.

[5] G. Dziuk, C. M. Elliott, *Eulerian finite element method for parabolic PDEs on implicit surfaces*, submitted.

[6] G. Dziuk, C. M. Elliott, *Eulerian level set method for partial differential equations on evolving surfaces*, in preparation.

Mathematical approaches to free boundary and interface problems

Charlie Elliott, Vanessa Styles

Free boundary problems are ubiquitous in models involving partial differential equations. The key idea is that besides seeking the solution of a system of PDEs for field variables one must also find the domain in which the equations hold. Thus one seeks an n-dimensional hypersurface Γ which may form part of the boundary of a domain $\Omega \in \mathbb{R}^{n+1}$ or be an interface which separates such a domain Ω into subdomains. Inherently these are nonlinear problems. Mathematical approaches to such problems have to deal with this nonlinearity and give a good notion of solution. Generally they vary in the way the hypersurface Γ is represented; for example

- The problem may be reformulated onto fixed domains using a coordinate transformation. This is a typical approach to proving local existence and uniqueness results for evolving surfaces in fluid dynamics.
- Integral equation methods have been used for reformulating the Stefan problem for the freezing of a pure material.
- Complex variable methods may be used to reformulate the problem in a number of ways when the PDE is Laplace's equation. These have been particularly useful in Hele-Shaw flow problems.

- The surface Γ may be defined as a level set of a function which within the bulk domain satisfies a degenerate nonlinear PDE which is already part of the model. For example, the two phase Stefan problem for freezing pure materials may be formulated as a degenerate nonlinear PDE for the temperature whose zero level set defines the phase change boundary.
- The problem is formulated variationally with an inequality constraint on the class in which the solution is sought. The free boundary is then the interface between the sub-domains where there is strict inequality and equality. For example, the obstacle problem for membranes is of this kind.
- The surface Γ is sought as a level set of an auxiliary function created to express the equations defining the surface. This is the basis of the *level set* method.
- The surface Γ is treated explicitly either as a graph or parametrically.

In these talks we surveyed several of these approaches. References on mathematical approaches to free boundary problems together with recent conference proceedings are appended to this abstract.

References

[1] P. Colli, C. Verdi and A. Visintin (editors) *Free boundary problems: Theory and applications* ISNM **147** Birkhauser (2004)

[2] J. Crank, *Free and moving boundary problems*, Oxford Science Publications Clarendon Press Oxford(1984) 424 pp

[3] C.M. Elliott and J.R. Ockendon) *Weak and variational methods for moving boundary problems*. Pitman, London 213 pp (1982).

[4] I. Figueiredo, J.F. Rodrigues and L. Santos (editors) *Free boundary problems: Theory and applications* ISNM **154** Birkhauser (2007)

[5] A. Friedman *Variational principles and free boundary problems* J. Wiley (1982)

[6] D. Kinderlehrer and G. Stampacchia *An introduction to variational inequalities and their application* Academic Press (1980)

[7] A. M. Meirmanov *The Stefan problem* De Gruyter Expositions in Mathematics **3** Walter de Gruyter Berlin New York (1992)

[8] J. F. Rodrigues *Obstacle problems in mathematical physics* North-Holland Mathematical Studies **134** North-Amsterdam New York Holland (1987)

[9] S. Osher and R. Fedkiw *Level set methods and dynamic implicit surfaces* Applied Mathematical Sciences **153** Springer (2003)

[10] J.A. Sethian *Level set methods and fast marching methods* Cambridge Monographs Applied and Computational Mathematics **3** Cambridge (1999)

Practical aspects in material design

Heike Emmerich

Many desirable properties of a material are determined by its micro structure. Thus contributing to a precise understanding of micro structure evolution in materials processing is a great challenge to the newly emerging field of computational materials design. From point of view of mathematics this always requires

to solve an intriguing and numerically difficult to handle *Stefan* problem. During the last two decades the phase-field method could establish itself within the computational materials science community to tackle such Stefan problems via an implicit formulation overcoming their inherent numerical inaccessibility. Moreover, the phase-field method is a variational thermodynamic approach making use of the materials equilibrium phase diagrams and thus allowing to specify concrete materials system.

Micro structure evolution in materials science is usually characterized by two circumstances: First, the material sample as such is driven out of equilibrium, and, second, even more fundamental, at the microscale we can detect interfaces, which separate two in some sense physically unlike regions of the sample from each other. Due to the non-equilibrium condition one of this two regions or phases will grow at the cost of the other. Examples are phase separation by spinodal decomposition or nucleation and subsequent growth of the nucleus in the nourishing phase[1]. Another example which has often been discussed as a paradigmatic problem is that of dendritic solidification[2, 3, 4, 5]. The phenomenological description of these phenomena involves the definition of a precisely located interfacial surface on which boundary conditions are imposed. One of those boundary conditions typically yields a normal velocity at which the interface is moving. This is the so-called *sharp interface* approach, adopted both in analytical and numerical studies for a variety of contexts involving a moving boundary. The origin of such a description is often transparent, being obtained by symmetry arguments and common sense. Nevertheless the properties of sharp interface models can be quite subtle as in the case for dendritic growth. This is strongly coupled to the question of how to view the interfacial surface. Already when introducing the notion of a surface quantity Gibbs implicitly entertained the idea of a diffuse interface[6]: any density of an extensive quantity (e.g., the mass density) between two coexisting phases varies smoothly from its value in one phase to its value in the other. The existence of a transition zone, though microscopically of atomic extent, underlies this definition of surface quantities as given by Gibbs. In phase transition phenomena, this notion has been employed in the spirit of Landau and Khalatnikov[7], who were the first to introduce an additional parameter to label the different phases in their theory on the absorption of liquid helium. Essentially diffuse interface or phase-field modeling, as it appeared subsequently in the literature in the context of phase transition phenomena[8, 9], is connected to such an additional order parameter. Clearly phase field models have advanced numerical treatment as well as understanding of micro structure evolution phenomena in materials science since.

Even though quite a young approach to tackle such problems, they have been employed by different groups in quite different spirits. An overview of this issue can be found in [10, 11]. The efforts described therein have resulted into very elaborate model formulations [12] as well as very elaborate numerical implementations as e.g. described in [13], which by now allow to simulate the growth of a single dendritic microstructure by at the same time taking into account long range

transport fields in reasonable time and high resolution. Thereby such approaches constitute an important contribution to carry out the relevant parameter studies for computational materials design, i.e. the parameter studies which allow to understand the relation between processing parameters and microstructure evolution and - at best - successively also the materials properties at the macroscale of a material systems. This shows that there is an inherent challenge to computational materials design due to the nature of materials properties evolution in any processing step itself: The latter is essentially a multiscale dynamics, i.e. a dynamics where different evolution paths occurring at different length and time scales are strongly coupled to each other. On this background it is quite easy to understand that in the further development of the phase field method in the context of computational materials design a lot of activities are concerned with this 'scale-bridging' issue. Basically three ways have emerged in the community to do so. The first is to design innovative algorithms which coupled different computational techniques originally designed for complementary scales as e.g. a DLA (Diffusion Limited Aggregation) or LBA (Lattice Boltzmann Automata) schemes to a phase field model [14]. The second is to use advanced numerical techniques as multi-grid, adaptivity and parallelization to do fast computation for several scales based on a single model approach. I third possibility arises from analytics, i.e. rigorous homogenization methods where one identifies the most relevant dynamical processes at each scale and develops a scale-bridging model based on these via expansion techniques [15]. Apart from these 'scale-bridging' efforts, however, likewise noteworthy broader directions of further development of the phase-field method have emerged. One of it is the evolution of nanostructures in condensed matter systems: What's remarkable about this point is that due to the continuum field nature of the phase-field approach one would claim that it should not be valid in this region. However, due to the successes of continuum approaches in microfluidics it appears to be justifiable to proceed with phase-field models for phase transition problems of similar physical nature at this scale, as well. Indeed quite successful studies could be carried out already [16]. Also the idea to employ phase-field models to investigate heterogenous nucleation dynamics as described below as an example for a phase-field based study in materials science, is based upon this underlying physical picture:

As described in more detail in [17] in that context phase-field modeling can help to understand the nucleation of the peritectic phase on top of the properitectic phase in a peritectic material system, which is characterized by a phase diagram as given in Fig. 1, in more detail. The standard variational procedure to obtain the relevant model equations are outline in [10, 11, 17]. In agreement with experimental finding and molecular simulations but with a clear perspective to go beyond these, first studies with the phase-field method demonstrate illustratively, that the morphology of an underlying seed phase cannot be neglected when predicting the nucleation rate of a second phase on top of it.

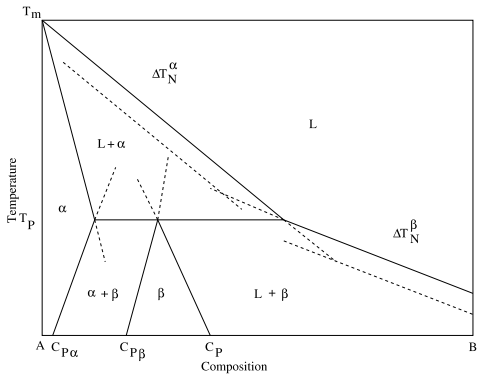

FIGURE 1. Schematic phase diagram of a peritectic alloy. C, concentration of impurity B; T_m, melting point of pure A; T_p, peritectic temperature. C_p, $C_{p\beta}$, and $C_{p\alpha}$ are the compositions of the liquid, β solid, and α solid that are in equilibrium at T_p. ΔT_N^α and ΔT_N^β are the nucleation undercoolings for α and β phases, respectively. Dashed lines are metastable extensions of the liquidus and solidus lines.

REFERENCES

[1] J.D. Gunton, M. San Miguel, P. Sahni: In *Phase Transitions and Critical Phenomena*, Vol.**8**, ed. by C. Domb, J.L. Lebowitz (Academic Press, London 1983), p. 267
[2] E. Ben-Jacob, N. Goldenfeld, J.S. Langer, G. Schön: Phys. Rev. A **29**, 330 (1984)
[3] B. Caroli, C. Caroli, B. Roulet: In *Solids Far From Equilibrium*, ed. by G. Godrèche (Cambridge University Press, Cambridge 1992), p. 155
[4] J. B. Collins, H. Levine: Phys. Rev. B **31**, 6119 (1985)
[5] J.S. Langer: Rev. Mod. Phys. **52**, 1 (1980)
[6] J.W. Gibbs: T. Conn. Acad. **2**, 382 (1873)
[7] D. ter Haar: *Collected Papers of Landau* (Gordon and Breach, Washington, DC, 1967)
[8] J.W. Cahn, J. E. Hilliard: J. Chem. Phys. **28**, 258 (1958)
[9] B.I. Halpering, P.C. Hohenberg, S. Ma: Phys. Rev. B **10**, 139 (1974)
[10] H. Emmerich, *The Diffuse Interface Approach in Material Science - Thermodynamic Concepts and Applications of Phase-Field Models,* Springer monograph, *Lecture Notes in Physics* **LNPm 73** (2003)
[11] H. Emmerich, *Advances of and by phase-field modeling in condensed matter physics*, review article invited to Advances in Physics, in preparation
[12] A. Karma, M. Plapp: Phys. Rev. Lett. **84**, 1740 (2000)
[13] J.–H. Jeong, N. Goldenfeld, J. Dantzig: Phys. Rev. E **64**, 041602 (2001)
[14] W. Miller, S. Succi, D. Mansutti: Phys. Rev. Lett. **86**, 3578 (2001)
[15] H. Emmerich, Ch. Eck, Cont. Mech. Thermodynamics **17**, 373 (2006)
[16] D. Kim et al., Nanotechnology **15**, 667 (2004)
[17] H. Emmerich, R. Siquieri, J. Phys.: Condens. Matter **18**, 11121 (2006)

Optimization problems and Cahn-Hilliard systems

Harald Garcke
(joint work with Luise Blank and Martin Butz)

The Cahn-Hilliard equation is the H^{-1}-gradient flow of the Ginzburg-Landau energy

$$E(u) = \int_\Omega \Big\{ \frac{\varepsilon\gamma}{2}|\nabla u|^2 + \tfrac{1}{\varepsilon}\psi(u) \Big\}\, dx\,.$$

Here γ and ε are positive constants, $\Omega \subset \mathbb{R}^n$ is a bounded domain and $\psi : \mathbb{R} \to \mathbb{R} \cup \{\infty\}$ is a double well potential.

Typical examples for ψ are

$$\begin{aligned} \psi(u) &= (1-u^2)^2\,, \\ \psi(u) &= \begin{cases} \psi_0(u) & \text{if} \quad u \in [-1,1]\,, \\ \infty & \text{elsewhere}\,, \end{cases} \end{aligned} \tag{1}$$

where $\psi_0 : \mathbb{R} \to \mathbb{R}$ is smooth and non-convex, e.g. $\psi_0(u) = \frac{1}{2}(1-u^2)$.

In the following we will focus on the obstacle case (1). In this case we obtain the variational inequality

$$\partial_t u = \Delta w \quad \text{for} \quad x \in \Omega,\, t > 0\,, \tag{2}$$

$$\gamma\varepsilon(\nabla u, \nabla(\chi - u))_{L^2} \geq (w - \tfrac{1}{\varepsilon}\psi_0'(u), \chi - u)_{L^2} \qquad \text{for all} \quad \chi \in H^1(\Omega)\,, \text{ with } |\chi| \leq 1\,,$$

where we also require homogeneous Neumann conditions for w.

For the spatial discretization we assume Ω to be a polyhedral domain. Then let $\mathcal{T}^h$ be a partitioning of Ω into disjoint open simplices with nodes J. Let $S^h := \{\chi \in C(\overline{\Omega}) \mid \chi \quad \text{is affine linear on the simplices}\}$ be the space of linear continuous finite elements and let $K^h := \{\chi \in S^h \mid |\chi| \leq 1 \quad \text{in} \quad \Omega\}$. Furthermore denote by $(.,.)^h$ the lumped mass inner product. Then given $u_h^0 \in S^h$ we seek for (u_h^n, w_h^n) for all $n = 1, \ldots, N$ such that

$$(u_h^n - u_h^{n-1}, \chi)^h + \tau(\nabla w_h^n, \nabla\chi) = 0 \quad \forall\, \chi \in S^h, \tag{3}$$

$$\varepsilon\gamma(\nabla u_h^n, \nabla(\chi - u_h^n)) \geq (w_h^n - \tfrac{1}{\varepsilon}\psi_0'(u_h^{n-1}), \chi - u_h^n)^h \quad \forall\, \chi \in K^h. \tag{4}$$

We propose to use a semi-smooth Newton method for the complementary formulation of (3), (4). Introducing a Lagrange multiplier μ for the inequality constraint we can rewrite (4) as

$$w^n = -\gamma\varepsilon\Delta u^n + \tfrac{1}{\varepsilon}\psi_0'(u^n) + \tfrac{1}{\varepsilon}\mu^n \tag{5}$$

together with

$$\begin{cases} \mu^n(|u^n| - 1) = 0\,, \\ |u^n| \leq 1\,, \\ \mu^n \leq 0 \text{ if } u^n = -1\,, \\ \mu^n \geq 0 \text{ if } u^n = 1 \end{cases} \tag{6}$$

which can be rewritten as (see also [4])

$$(7)\quad H(\mu^n, u^n) := \mu^n - c(\max(0, \tfrac{1}{c}\mu^n + (u^n - 1)) + \min(0, \tfrac{1}{c}\mu^n + (u^n + 1)) = 0 \quad \text{a.e.}.$$

We solve the system (4), (5) and (7) numerically with the help of a semi-smooth Newton method, which can be interpreted as an active set strategy.

With the help of an energy argument using the saddle point structure it is possible to show that the generalized Jacobians related to the mappings in (4), (5) and (7) are invertible and hence we can show that the semi-smooth Newton method converges locally superlinearly. In each time step typically only one or two Newton iterations are needed. We noticed that for the double obstacle Cahn-Hilliard problem as stated above c has to be chosen large enough in order to guarantee that no oscillations between the two active sets occur during the iterations. If this happens the Newton method might not converge globally. This can happen for other bilateral obstacle problems as well. More details on the semi-smooth Newton method for the Cahn-Hilliard equation will appear elsewhere [1].

Finally let us briefly discuss a few optimization problems in which Cahn-Hilliard equations or Cahn-Hilliard variational inequalities are relevant. We will focus on applications in which elastic effects play a role.

In this case we have to couple the system for (u, w) to the displacement field $\mathbf{u}$. Introducing the linearized strain tensor $\mathcal{E}(\mathbf{u}) = \frac{1}{2}(\nabla \mathbf{u} + \nabla \mathbf{u}^{\mathbf{T}})$, a suitable interpolation function c, the elasticity tensor C, the stress free strain $\overline{\mathcal{E}}$ and the elastic energy density

$$(8)\qquad W(u, \mathcal{E}(\mathbf{u})) = \tfrac{1}{2} c(u) C(\mathcal{E}(\mathbf{u}) - \overline{\mathcal{E}}) : (\mathcal{E}(\mathbf{u}) - \overline{\mathcal{E}})$$

we have to replace (2) by the following equation

$$(9)\qquad \partial_t u = \nabla \cdot (b(u) \nabla (w + W_{,u}(u, \mathcal{E}(\mathbf{u})))) + \gamma\, \mathbf{q} \cdot \nabla u$$

where b is the mobility and $\mathbf{q}$ is a given vector (the direction of the deposition flux). Given the stress tensor $\mathcal{S} = c(u) C(\mathcal{E}(\mathbf{u}) - \overline{\mathcal{E}})$, the displacement $\mathbf{u}$ solves the elasticity system

$$(10)\qquad \nabla \cdot \mathcal{S} = \nabla \cdot (c(u) C(\mathcal{E}(\mathbf{u}) - \overline{\mathcal{E}})) = 0.$$

This system is supplemented with the boundary conditions

$$(11)\qquad \mathcal{S} \cdot \mathbf{n} \;=\; g \quad \text{on} \quad \Gamma_1 \times [0, T]\,,$$

$$(12)\qquad \mathbf{u} \;=\; \mathbf{u}_D \quad \text{on} \quad (\partial\Omega \setminus \Gamma_1) \times [0, T]$$

where $\mathbf{u}_D$ are Dirichlet data and g are outer forces on a part $\Gamma_1 \subset \partial\Omega$. For background material we refer to [3].

Controlled crystal growth of quantum dots. In heteroepitaxial growth of thin solid films a solid film growths on a substrate. An elastic mismatch between substrate and film results in elastic stresses. Now atoms diffuse on the surface in order to reduce the elastic and the surface energy of the film. It is by now well established that a uniform film can become unstable and islands can form. There

is the hope that the formation of these islands can be used to produce quantum-dot-based devices for quantum computing or laser technology. It is a challenge to control the formation of islands such that a large number of spatially ordered islands ("quantum dots") form. There is the possibility to control the growth by a design of the substrate or a local variation of the mismatch between film and substrate. Here theoretical modeling, efficient numerical simulations and the development of fast optimization algorithms will play an important role.

Ripening processes in alloys (Ostwald ripening). In a binary alloy which is quenched underneath a critical temperature phases with different concentrations of the alloy components form. After the initial formation of regions with different phases typically many small particles are present. Due to diffusion processes smaller particles disappear and larger particles grow ("inverse Robin-Hood-phenomenon"). For most practical applications this is not desirable as optimal properties of the alloys rely on distributed phases. It is therefore desirable to control the ripening process in such a way that the growth slows down or even stops. It is possible to control the growth by outer stresses or one can try to find optimal parameters in the elasticity system in order to design new alloys with desirable properties.

Possible control problems include

Boundary control of the phase distribution.

If we want to obtain a given distribution of phase u_w at a time $T > 0$ and if we are allowed to control the outer stress g on a part $\Gamma_1 \subset \partial\Omega$ we need to minimize e.g. the functional

$$\mathcal{J}_1(u,g) = \tfrac{1}{2}\int_\Omega (u-u_w)^2(T,x)dx + \frac{\alpha}{2}\int_0^T \int_{\Gamma_1} g^2(x,t)d\mathcal{H}^{n-1}(x)dt \tag{13}$$

($\mathcal{H}^{n-1}$ denotes the $(n-1)$-dimensional surface measure) subject to the extended Cahn-Hilliard equations.

Minimize/Maximize interfacial energy.

Often in applications in materials science the interfacial energy is a quantity that one wants to optimize. Given the interfacial energy $\int\limits_\Omega \{\frac{\varepsilon\gamma}{2}|\nabla u|^2 + \frac{1}{\varepsilon}\psi(u)\}$, we would need to replace the cost functional (13) by

$$\mathcal{J}_2(u,g) = \pm\int\limits_\Omega \{\tfrac{\varepsilon\gamma}{2}|\nabla u|^2 + \tfrac{1}{\varepsilon}\psi(u)\}(T,x)dx + \frac{\alpha}{2}\int_0^T \int_{\Gamma_1} g^2(x,t)d\mathcal{H}^{n-1}dt \tag{14}$$

to come close to extremas of the interfacial energy. In fact in several applications one wants to avoid coarsening of the phase regions. This can be obtained by a control that aims to keep a high interfacial energy. In other cases e.g. in grain growth, which is governed by an Allen-Cahn system, one would like to keep the interfacial energy low.

References

[1] L. Blank, M. Butz, and H. Garcke, *On a semi-smooth Newton method for the Cahn-Hilliard variational inequality*, in preparation.

[2] J. F. Blowey and C. M. Elliott, *The Cahn-Hilliard gradient theory for phase separation with non-smooth free energy*, Part I: Mathematical analysis. European J. of Appl. Math. **2** (1991), pp. 233–280.

[3] H. Garcke, *Mechanical effects in the Cahn-Hilliard model: A review on mathematical results* in "Mathematical Methods and Models in phase transitions", ed.: Alain Miranville, Nova Science Publ. (2005), 43–77

[4] M. Hintermüller, K. Ito, and K. Kunisch, *The primal-dual active set strategy as a semismooth Newton method*, SIAM J. Optim. **13** (2002), no. 3, 865–888.

Control Issues in Magnetohydrodynamics

Roland Griesse

(joint work with Amnon J. Meir, Karl Kunisch)

Magnetohydrodynamics, or MHD, deals with the mutual interaction of electrically conducting fluids and magnetic fields. The coupling between fluid motion and the electromagnetic quantities arises from the following three phenomena:

(1) The relative movements of a conducting fluid and a magnetic field induce an electromotive force to the effect that an electric current develops in the fluid.
(2) This current in turn induces a magnetic field.
(3) The magnetic field interacts with the current in the fluid and exerts a Lorentz force on the fluid.

The Lorentz force offers a unique possibility of generating a volume force in the fluid and hence to control its motion in a contactless fashion and without any mechanical interference.

The MHD system consists of the Navier-Stokes equation with Lorentz force, and a simplified form of Maxwell's equations, with the displacement current neglected. The dependent variables are the fluid velocity $\boldsymbol{u}$ and its pressure p, plus the electric current density $\boldsymbol{J}$, the electric field $\boldsymbol{E}$ and the magnetic induction $\boldsymbol{B}$. We also incorporate the fluid's temperature T below. In the stationary case, the MHD system is given by (see, e.g., [1, 9])

$$\text{(1a)} \qquad \nabla \cdot \boldsymbol{J} = 0, \qquad \nabla \times \boldsymbol{E} = 0,$$

$$\text{(1b)} \qquad \nabla \cdot \boldsymbol{B} = 0, \qquad \nabla \times (\mu^{-1}\boldsymbol{B}) = \boldsymbol{J},$$

$$\text{(1c)} \qquad \boldsymbol{J} = \sigma\,(\boldsymbol{E} + \boldsymbol{u} \times \boldsymbol{B}).$$

The electric field $\boldsymbol{E}$ is usually expressed as the negative gradient of the electric potential ϕ, $\boldsymbol{E} = -\nabla\phi$, and this is inserted into (1c).

The fluid's velocity is governed by the incompressible Navier-Stokes system (Boussinesq approximation) with Lorentz and buoyancy forces

$$\varrho\,(\boldsymbol{u}\cdot\nabla)\boldsymbol{u} - \eta\,\Delta\boldsymbol{u} + \nabla p = \boldsymbol{J}\times\boldsymbol{B} + \varrho\,[1-\beta(T-T_{\mathrm{ref}})]\,\boldsymbol{g}, \tag{2a}$$

$$\nabla\cdot\boldsymbol{u} = 0. \tag{2b}$$

Here and throughout, μ denotes the magnetic permeability of the matter occupying a certain point in space, and ϱ, η and σ denote the fluid's density, viscosity and conductivity. In the buoyancy term, T_{ref} denotes a reference temperature, β is the thermal expansion coefficient, and $\boldsymbol{g}$ the acceleration of gravity. The temperature is governed by the convection-diffusion equation

$$-\kappa\,\Delta T + \varrho\,c_p(\boldsymbol{u}\cdot\nabla)T = \sigma^{-1}|\boldsymbol{J}|^2, \tag{3}$$

where κ is the fluid's thermal conductivity, and c_p is its specific heat at constant pressure. The right hand side in (3) accounts for Joule (Ohmic) heating of the fluid due to its electrical resistance.

System (1)–(3) is to be closed by appropriate boundary conditions for the fluid velocity $\boldsymbol{u}$, the current-potential pair $(\boldsymbol{J},\phi)$ and the temperature T. The magnetic induction $\boldsymbol{B}$ extends outside the domain occupied by the fluid and vanishes at infinity.

MHD phenomena are relevant in a number of industrial applications, such as melting and casting processes of metals, as well as crystal growth. In some of these applications, a free fluid surface is present, possibly in addition to a free liquid–solid interface. For the characterization of the free surface, we introduce the fluid's total stress tensor

$$\mathcal{T} = -pI + \eta\left(\nabla\boldsymbol{u} + (\nabla\boldsymbol{u})^{\top}\right),$$

where I is the identity tensor. The stress tensor of the surrounding atmosphere (if at rest) is simply $-p_{\mathrm{atm}}I$.

The Laplace-Young equation states that the jump of the normal stresses across the free surface is equal to the product of the surface tension coefficient γ and the curvature of the interface. Assuming that the free surface can be described as the graph of a function H, the surface curvature is given by

$$\nabla'\cdot\frac{\nabla' H}{\sqrt{1+|\nabla' H|^2}},$$

where $\nabla'\cdot(\cdot)$ and $\nabla'(\cdot)$ are the surface divergence and gradient, respectively. The Laplace-Young equation yields the condition

$$-\gamma\nabla'\cdot\frac{\nabla' H}{\sqrt{1+|\nabla' H|^2}} + p_{atm} = -(\mathcal{T}\boldsymbol{n})\cdot\boldsymbol{n} = p - \eta\left(\left(\nabla\mathbf{u} + (\nabla\mathbf{u})^{\top}\right)\boldsymbol{n}\right)\cdot\boldsymbol{n}. \tag{4}$$

Note that in (4), $\boldsymbol{n}$ denotes the outward pointing normal vector to the surface, and we abuse notation since the right hand side is to be evaluated on the free surface rather than on the domain of the function H. (4) is a second-order partial differential equation which, together with the associated conditions (5)–(6), determines

the location of the free surface. As a boundary condition for H we have [2]

$$\frac{\nabla' H}{\sqrt{1+|\nabla' H|^2}} \cdot \boldsymbol{n}' = \cos\alpha(T). \tag{5}$$

Here $\boldsymbol{n}'$ is the planar outward pointing unit normal vector to the domain of definition of H. Condition (5) specifies the contact angle α, which is in general temperature-dependent. It is also a material property which may be affected by surface treatments. The constraint

$$\int_{\Gamma_f} H\, dx = 0 \tag{6}$$

accounts for the conservation of fluid volume. Note that here we continue to employ the underlying assumption from the Boussinesq approximation, that the density is constant except in the buoyancy term.

The jump of the tangential stresses across the free surface stems from the gradient of the surface tension γ. We account for variations in γ with temperature which give rise to the so-called Marangoni effect, which can be significant in crystal growth problems [7]. We obtain

$$\mathcal{T}\boldsymbol{n} - \big((\mathcal{T}\boldsymbol{n})\cdot\boldsymbol{n}\big)\boldsymbol{n} = \frac{d\gamma}{dT}\big(\nabla T - (\nabla T\cdot\boldsymbol{n})\,\boldsymbol{n}\big). \tag{7}$$

Note that (7) yields non-trivial conditions only in directions perpendicular to the surface normal $\boldsymbol{n}$. As the final condition, we impose the non-penetration constraint

$$\mathbf{u}\cdot\boldsymbol{n} = 0 \tag{8}$$

on the free surface.

Depending on the type of variables or parameters at one's disposal, the optimization of processes governed by the free surface MHD system above lead to optimal control problems or shape optimization problems. Controllable quantities include

- heat sources, modeled as additional right hand sides in (3), or as boundary conditions,
- rotation speeds of the fluid container,
- the location, strength and configuration of applied magnetic fields $\boldsymbol{B}_0$, which are added to the induced field $\boldsymbol{B}$ in (1c) and (2a),
- the geometry of the domain.

For details and examples we refer to [5, 11, 10, 12, 8, 3, 4, 6].

References

[1] P. A. Davidson. *An Introduction to Magnetohydrodynamics*. Cambridge University Press, Cambridge, 2001.

[2] R. Finn. Capillary surface interfaces. *Notices of the AMS*, 46(7):770–781, 1999.

[3] R. Griesse and K. Kunisch. Optimal control for a stationary MHD system in velocity–current formulation. *SIAM Journal on Control and Optimization*, 45(5):1822–1845, 2006.

[4] R. Griesse and A. J. Meir. Modeling of an MHD free surface problem arising in CZ crystal growth. In I. Troch and F. Breitenecker, editors, *5th IMACS Symposium on Mathematical Modelling—5th MATHMOD Vienna*, ARGESIM Reports, 2006. ISBN 3-901608-30-3.

[5] M. Gunzburger, E. Ozugurlu, J. Turner, and H. Zhang. Controlling transport phenomena in the Czochralski crystal growth process. *Journal of Crystal Growth*, 234:47–62, 2002.
[6] M. Hinze and S. Ziegenbalg. Optimal control of the free boundary in a two-phase Stefan problem. *J. Comput. Phys.*, 223:657-684 (2007).
[7] V. Kumar, B. Basu, S. Enger, G. Brenner, and F. Durst. Role of Marangoni convection in Si-Czochralski melts—Part I: 3d predictions with crystal rotation. *Journal of Crystal Growth*, 255:27–39, 2003.
[8] M. Metzger. Optimal control of crystal growth processes. *Journal of Crystal Growth*, 23(1–2):210–216, 2001.
[9] J. A. Shercliff. *A Textbook of Magnetohydrodynamics*. Pergamon Press, Oxford, 1965.
[10] J. Turner. Modelling control of crystal growth processes. *Computers and Mathematics with Applications*, 48(7–8):1231–1243, 2004.
[11] A. Voigt and K.-H. Hoffmann. Control of Czochralski crystal growth. In *Optimal control of complex structures (Oberwolfach, 2000)*, volume 139 of *Internat. Ser. Numer. Math.*, pages 259–265. Birkhäuser, Basel, 2002.
[12] C. Wang, H. Zhand, T. Wang, and L. Zheng. Solidification interface shape control in a continuous Czochralski silicon growth system. *Journal of Crystal Growth*, 287(2):252–257, 2006.

Inequality Constraints in PDE-constrained optimization

Michael Hintermüller

In recent years significant progress in the theoretical as well as numerical understanding of pointwise inequality constraints in optimization problems subject to partial differential equations (PDE-constrained optimization, for short) was made. According to increasing degree of difficulty from an optimization-theoretic (and also numerical) point of view we first address PDE-constrained optimization model problems subject to pointwise control-constraints:

$$\begin{aligned} &\text{minimize} \quad J(y,u) = \tfrac{1}{2}\|y-y_d\|_{L^2}^2 + \tfrac{\alpha}{2}\|u\|_{L^2}^2 \text{ over } (y,u) \in H^1(\Omega)\times L^2(\Omega), \\ &\text{s.t.} \quad Ay + g(y) = Bu \text{ in } \Omega, \quad y = 0 \text{ on } \Gamma = \partial\Omega, \\ &\qquad u \in U_{\rm ad} = \{u \in L^2(\Omega) \ : \ a(\mathrm{x}) \le u(\mathrm{x}) \le b(\mathrm{x}) \text{ f.a.a. x in } \Omega\}, \end{aligned} \tag{1}$$

where $\alpha > 0$, $y_d \in L^2(\Omega)$ is the desired state, A is a second order elliptic partial differential operator, $B \in \mathcal{L}(L^2(\Omega))$, g is sufficiently smooth and monotonous, $a, b \in L^2(\Omega)$, $a < b$, are given bounds. The domain Ω is assume to be bounded with sufficiently smooth boundary $\Gamma = \partial\Omega$. Then we consider obstacle problems

$$\begin{aligned} &\text{minimize} \quad J(y) = \tfrac{1}{2}\|\nabla y\|_{L^2}^2 - \langle f, y\rangle_{H^{-1},H_0^1} \\ &\text{s.t.} \quad y \in K := \{v \in H_0^1(\Omega) : y \le \psi \text{ a.e. in } \Omega\}, \end{aligned} \tag{2}$$

where $f \in H^{-1}(\Omega)$ and $\psi \in H^1(\Omega)$, $\psi|_\Gamma > 0$, are given. Next, with $W = H^2(\Omega) \cap H_0^1(\Omega)$, state constrained problems of the type

$$\begin{aligned} &\text{minimize} \quad J(y,u) = \tfrac{1}{2}\|y-y_d\|_{L^2}^2 + \tfrac{\alpha}{2}\|u\|_{L^2}^2 \text{ over } (y,u) \in W\times L^2(\Omega), \\ &\text{s.t.} \quad Ay = Bu \text{ in } \Omega, \quad y \in Y_{\rm ad} = \{y \in H_0^1(\Omega) : \ y \le \psi \text{ a.e. in } \Omega\} \end{aligned} \tag{3}$$

are studied. Finally, we address so-called mathematical programs with complementarity constraints (for short MPCC) in function space:

(4)
$$\begin{aligned} &\text{minimize} \quad J(y,u) = \tfrac{1}{2}\|y - y_d\|_{L^2}^2 + \tfrac{\alpha}{2}\|u\|_{L^2}^2 \text{ over } (y,u,\lambda) \in H_0^1(\Omega) \times L^2(\Omega)^2, \\ &\text{s.t.} \quad Ay - \lambda = Bu + f \text{ in } \Omega, \quad y \geq 0, \quad \lambda \geq 0, \quad y\,\lambda = 0 \text{ a.e. in } \Omega. \end{aligned}$$

Concerning (1), here we will focus on numerical solution procedures. It turned out that the primal-dual active set strategy (pdAS) is a very efficient solution method; see [1]. In particular, in [1] the following notion of generalized (Newton) differentiability in function space is introduced:

Definition. *The mapping $F : D \subset X \to Z$, with X, Z Banach spaces, is generalized (or Newton) differentiable in $U \subset D$, if there exists a family of mappings $G : U \to \mathcal{L}(X, Z)$ such that*

$$\text{(A)} \qquad \lim_{h \to 0} \frac{1}{\|h\|_X} \|F(x+h) - F(x) - G(x+h)h\|_Z = 0 \quad \forall x \in U.$$

With this definition, it can be shown that pdAS is equivalent to a semismooth Newton method (SSN) and, thus, converges locally at a superlinear rate. Moreover, the method fulfills a mesh independence principle.

Similar results are not immediately available for (2) and (3) which is due to the lack of certain smoothing properties or poor multiplier regularity, respectively. Using a Moreau-Yosida-based regularization, however, allows to approximate the original problem by a sequence of regularized problems which can again be solved very efficiently by SSN. Moreover, a function space theory and mesh independence considerations are then available again. For (2) the regularization operates by replacing J by

$$J_\gamma(y) = J(y) + \frac{1}{2\gamma}\|(\bar{\lambda} + \gamma(y - \psi))_+\|_{L^2}^2,$$

with $\gamma > 0$ the regularization parameter, $(\cdot)_+ = \max(0, \cdot)$ in the pointwise sense, and $\bar{\lambda} \geq 0$, $\bar{\lambda} \in L^2(\Omega)$, is a shift-parameter which, if appropriately chosen, yields feasibility of the regularized solution with respect to the constraints in (2). By employing the regularization, the explicit constraint $y \leq \psi$ is replaced by an implicit one. It can be shown that the solution y_γ to the regularized problem converges strongly in $H_0^1(\Omega)$ to y^*, the solution of the original problem (2). Due to the structural properties implied by the regularization a path-following technique with γ as the path-parameter can be derived. This results in an efficient updated procedure for γ; see [2]. A similar strategy works well also for (3); see [3].

Finally, MPCC will be considered. First we note that due to the structure of the feasible set classical constraint qualifications such as the Mangasarian-Fromovitz constraint qualification do not hold true. As a result the existence of Lagrange multipliers for characterizing first order optimality cannot be derived from standard results. We highlight two techniques for deriving first order necessary conditions, one based on a possible bilevel structure of the problem and a more general second one utilizing suitable relaxations of the feasible set such that classical results

for multipliers existence for the regularized problems can be applied. The resulting first order conditions, which are obtained after passage to the limit, resemble strong stationarity well-known from finite dimensional MPCCs.

Theorem: *For an optimal solution* (y^*, u^*, λ^*) *of* (4) *there exist multipliers* $p^* \in H_0^1(\Omega)$ *and* $\mu^* \in H^{-1}(\Omega)$ *satisfying*

$$\begin{aligned} A^*p^* - \mu^* + \nabla_y J(y^*, u^*) &= 0, \\ \nabla_u J(y^*, u^*) - B^\star p^* &= 0, \\ p^*\lambda^* = 0, \quad 0 \le -p^*|_{\mathcal{B}^*} \perp \lambda^*|_{\mathcal{B}^*} &\ge 0, \ a.e., \\ 0 \le \mu^*|_{\mathcal{B}^*} \perp y^*|_{\mathcal{B}^*} &\ge 0, \\ Ay^* - \lambda^* - Bu^* - f &= 0, \quad \Theta(y^*, \lambda^*) = 0 \ a.e., \end{aligned}$$

where $\mathcal{B}^* = \{y^* = 0 \wedge \lambda^* = 0\}$ and Θ denotes a NCP-function, i.e., it satisfies

$$\Theta(r, s) = 0 \quad \Longleftrightarrow \quad r \ge 0, \ s \ge 0, \ r\, s = 0.$$

References

[1] M. Hintermüller, K. Ito, and K. Kunisch, *The primal-dual active set strategy as a semi-smooth Newton method*, SIAM J. Optim., **13** (2003), 865–888.

[2] M. Hintermüller and K. Kunisch, *Path-following methods for a class of constrained minimization problems in function space*, SIAM J. Optim., **17** (2006), 159–187.

[3] M. Hintermüller and K. Kunisch, *Feasible and non-interior path-following in constrained minimization with low multiplier regularity*, SIAM J. Control Optim., **45** (2006), 1198–1221.

Concepts of pde constrained optimization

Michael Hinze

Pde–constrained optimization problems can be written in the form

$$(P) \qquad \min_{u \in U_{\rm ad}, y \in Y_{\rm ad}} J(y, u) \text{ s.t. } PDE(y) = B(u),$$

where J denotes a cost functional which expresses the control goal mathematically, y denotes the state, u the control, and B an appropriately chosen control operator. Control and state are coupled through $PDE(y) = B(u)$, which frequently also is called state equation. From the optimization point the problem (P) forms an infinite–dimensional optimization problem in Banach spaces, but admits a special structure.

In what follows it is convenient to define $PDE(y, u) := PDE(y) - B(u)$ with $PDE : Y \times U \to Z^*$ sufficiently smooth, and to assume that $B : U \to Z^*$ is a bounded, linear control operator. Here, Y denotes a Banach space of states, U the Hilbert space of controls, and Z^* the range space of the pde. In (P) one further requires $U_{\rm ad}, Y_{\rm ad} \subset U, Y$ closed and convex, so that weak limits of sequences of elements of these subsets are contained in these subsets, and .

Examples. Now let $PDE(y,u)=0 \Longleftrightarrow$

$$\begin{aligned}\left(\frac{\partial y}{\partial t}+\right)\mathcal{A}y+\mathcal{N}(y) &= \mathcal{B}u \text{ in } Z^*\\ (y(0) &= y_0 \text{ in } H,)\end{aligned}$$

where in the case of time–dependent problems H denotes the Hilbert space of initial values. Typical examples of pdes include

- Poisson, Heat equation: $\mathcal{A}:=-\Delta$,
- Burgers: $\mathcal{A}:=-\Delta$, $\mathcal{N}(y):=yy'$,
- Ignition (Bratu): $\mathcal{A}:=-\Delta$, $\mathcal{N}(y):=-\delta e^y$, $\delta>0$,
- Navier–Stokes: $\mathcal{A}:=-P\Delta$, $\mathcal{N}(y):=P[(y\nabla)y]$, P Leray projector,
- Boussinesq Approximation: $\mathcal{A}:=\begin{bmatrix}-P\Delta & -Gr\vec{g}\\ 0 & -\Delta\end{bmatrix}$, $\mathcal{N}(y)=\mathcal{N}(v,\theta):=\begin{bmatrix}P[(v\nabla)v]\\ (v\nabla)\theta\end{bmatrix}$,

frequently used cost functionals $J: Y\times U\to\mathbb{R}$ are given by

- Tracking–type: $J(y,u)=\frac{1}{2}\|y-z\|^2_{L^2(H)}+\frac{\alpha}{2}\|u\|^2_U$.
- Vorticity–type: $J(y,u)=\frac{1}{2}\|curly\|^2_{L^2(\Omega)}+\frac{\alpha}{2}\|u\|^2_U$
- Force: $J(y,p,u)=\int_S -\eta\cdot(\nu\nabla y-pI)\cdot edS+\frac{\alpha}{2}\|u\|^2_U$,

common control operators B are of the form $\mathcal{B}$:

- Distributed control: $\mathcal{B}u=u$ for $u\in L^2(Q)$, say,
- Boundary control: $\mathcal{B}u=\gamma^*u$ for $u\in L^2(\Gamma)$, say,
- Amplitudes: $\mathcal{B}u=\sum u_if_i$ for $u\in L^2(0,T)^m$, say,

and practically important constraints are given by

- Bound constraints: $U_{\rm ad}=\{u; a\le u\le b \text{ a.e. in } \Omega\}$, $Y_{\rm ad}=\{y; c\le y\le d \text{ a.e. in } \Omega\}$,
- Constraints on derivatives: $Y_{\rm ad}=\{y;|\nabla y|\le d \text{ a.e. in } \Omega\}$.

Structure: The reduced functional. Frequently, $PDE(y,u)=0$ admits a unique solution for $u\in U$. Thus, the state is a function of the control, i.e. $y=y(u)$ and the pde constrained optimization problem (P) becomes

$$(\hat{P})\quad \min_{u\in U_{\rm ad}}\hat{J}(u):=J(y(u),u) \text{ s.t. } PDE(y(u),u)=0 \text{ in } Z^*, \text{ and } y(u)\in Y_{\rm ad}.$$

For the Derivatives of $\hat{J}$ we obtain by the chain rule

$$\hat{J}'(u)=J_y(y(u),u)y'(u)+J_u(y(u),u).$$

Also frequently $PDE_y(y(u),u): Y\to Z^*$ admits a bounded inverse, so that, using the implicit function theorem, we obtain an expression for $y'(u)$;

$$PDE(y(u),u)=0\Longrightarrow \quad y'(u)=-PDE_y(y(u),u)^{-1}PDE_u(y(u),u),$$

so that application of the adjoint calculus yields

$$\hat{J}'(u)=-PDE_u(y(u),u)^*PDE_y(y(u),u)^{-*}J_y(y(u),u)+J_u(y(u),u).$$

Structure: Derivatives and adjoints. Let us define the so called adjoint variable

$$p := PDE_y(y(u),u)^{-*} J_y(y(u),u),$$

which allows to express the derivative of $\hat{J}$ in the form

$$\hat{J}'(u) = -PDE_u(y(u),u)^* p + J_u(y(u),u) \equiv \mathcal{B}^* p + J_u(y(u),u) \in U^*.$$

In order to provide an expression for the second derivative of $\hat{J}$ we assume $J(y,u) = J_1(y) + J_2(u)$ and differentiate $PDE(y,u) = 0$ one more time to obtain an expression for $y''(u)$. The chain rule then gives

$$\begin{aligned}\langle \hat{J}''(u)\delta u, \delta v\rangle_{U^*,U} = {} & \langle J_{yy}(x)y'(u)\delta u, y'(u)\delta v\rangle_{Y^*,Y} + \\ & + \langle PDE_{yy}(y,u)(y'(u)\delta u, y'(u)\delta v), p\rangle_{Z^*,Z} + \langle J_{uu}(u)\delta u, \delta v\rangle_{U^*,U}.\end{aligned}$$

Using the representation of y' then yields

$$\begin{aligned}\hat{J}''(u) = {} & PDE_u(y,u)^* PDE_y(y,u)^{-*} \{J_{yy}(y,u)(\bullet,\bullet) + \\ & + \langle PDE_{yy}(y,u)(\bullet,\bullet), p\rangle_{Z^*,Z}\} PDE_y(y,u)^{-1} PDE_u(y,u) + J_{uu}(y,u).\end{aligned}$$

Structure: Optimality conditions. Optimality conditions for problem $(\hat{P})$ may be deduced from [1]; Let $u \in U_{\mathrm{ad}}$ denote a solution of the pde constrained optimization problem and let Y_{ad} have nonempty interior. Then there exists some $\mu \in Y^*$ and a real number $\lambda \geq 0$ such that

$$\lambda + \|\mu\|_{Y^*} > 0, \quad \langle \mu, z - y(u)\rangle_{Y^*,Y} \leq 0 \text{ for all } z \in Y_{\mathrm{ad}},$$

and

$$\begin{aligned}\langle \lambda J_u(y,u) - PDE_u(y,u)^* PDE_y(y,u)^{-*}(\lambda J_y(y,u) + \mu), v - u\rangle_{U^*,U} \geq 0 \\ \text{for all } v \in U_{\mathrm{ad}}.\end{aligned}$$

If some $u^0 \in U_{\mathrm{ad}}$ exists such that

$$y(u) - PDE_y(y,u)^{-1} PDE_u(y,u)^*(u^0 - u) \in \operatorname{int} Y_{\mathrm{ad}} \text{ (Slater condition)},$$

then $\lambda = 1$ can be chosen.

Modern algorithmic concepts exploit the structure of the optimality conditions. For details we refer to the contributions of Michael Hintermüller and Karl Kunisch.

Structure conserving discretization. Concerning discrete concepts it is a general rule to transfer as much structure of the continuous problem as possible to its discrete counterpart. And one also should only discretize those variables which need to be discretized in order to compute numerical approximations of solutions to the continuous problem. Discretization should be *minimal invasive*, so to say. For problem $(\hat{P})$ the following discrete version obeys these rules;

$$(\hat{P}_h) \quad \min_{u \in U_{\mathrm{ad}}} \hat{J}_h(u) := J(y_h(u),u) \text{ s.t. } PDE_h(y_h(u),u) = 0 \text{ in } Z_h^*, \text{ and } y_h(u) \in Y_{\mathrm{ad}}^h.$$

In this approach, the pde is discretized and only state spaces are substituted by appropriate finite–dimensional counterparts. The controls are not discretized

(explicitely). This concept is developed in [5], details can be found in [6, Chapter 3]. Research on numerical analysis for state constrained problems, i.e. $Y_{\rm ad}$ a proper subset of Y, is ongoing, see [2, 3, 4].

References

[1] Casas, E.: *Boundary control of semilinear elliptic equations with pointwise state constraints*, SIAM J. Cont. Optim. **31**, 993–1006 (1993).

[2] Casas, E., Mateos, M.: *Uniform convergence of the FEM. Applications to state constrained control problems*. Comp. Appl. Math. **21** (2002).

[3] Deckelnick, K., Hinze, M.: *Convergence of a finite element approximation to a state constrained elliptic control problem*, MATH-NM-01-2006, Institut für Numerische Mathematik, TU Dresden (2006).

[4] Deckelnick, K., Hinze, M.: *A finite element approximation to elliptic control problems in the presence of control and state constraints*, Hamburger Beiträge zur Angewandten Mathematik, Preprint HBAM2007-01 (2007).

[5] Hinze, M.: *A variational discretization concept in control constrained optimization: the linear-quadratic case*, J. Computational Optimization and Applications **30**, 45-63 (2005).

[6] Hinze, M., Pinnau, R., Ulbrich, M., and Ulbrich, S: *Modeling and Optimization with Partial Differential Equations*, Lecture Notes of the Autumn School, Universität Hamburg (2005).

Semi-smooth Newton Methods for Variational Problems with Simple Constraints

Karl Kunisch

We consider three prototypical examples for a control constrained optimal control problem.

$$(P\,1)\qquad \begin{cases} \min\, Q(y) + \frac{\alpha}{2}|u|^2 \\ -\Delta y = u \text{ in } \Omega \\ y = 0 \text{ on } \partial\Omega \\ u \le \psi, \quad u \in L^2(\Omega), \end{cases}$$

where Q is a quadratic functional on $L^2(\Omega)$, bounded from below, $\alpha > 0, \psi \in L^p(\Omega), p > 2$. Further a variational inequality

$$(P\,2)\qquad \begin{cases} \min \frac{1}{2}\int_\Omega |\nabla y|^2\,dx - \int_\Omega f\,y\,dx \\ y \le \psi,\, y \in H_0^1(\Omega), \quad \psi \in H^2(\Omega), \quad \psi|\partial\Omega \le 0 \end{cases}$$

and a state-constrained optimal control problem

$$(P\,3)\qquad \begin{cases} \min\, Q(y) + \frac{\alpha}{2}|u|^2 \\ -\Delta y = u \text{ in } \Omega \\ y = 0 \text{ on } \partial\Omega \\ y \le \psi \text{ in } \Omega. \end{cases}$$

From the point of duality theory these three problems are quite different. While for (P 1) the existence of a Lagrange multiplier $\lambda \in L^2(\Omega)$ associated to the constrained $u \leq \psi$ can easily be argued, e.g. as a consequence of surjectivity of the constraint operator, the existence of a Lagrangian associated to $y \leq \psi$ in (P 2) requires a sophisticated approximation technique and the multiplier associated to $y \leq \psi$ in (P 3) is only a measure. Accordingly numerical methods, considered in function space should reflect this difference of regularity of the multipliers. We note that necessary and sufficient optimality condition for (P 1) can be expressed as

$$F(u) = \alpha u - p + \max(0, p - \alpha\psi),$$

where $p = \Delta^{-1}Q'(-\Delta^{-1}u)$.

This mapping is Newton-differentiable from $L^2(\Omega)$ to itself, in the following sense:

Definition $F : D \subset X \to Z$ is Newton differentiable in $U \subset D$, if there exists $G : U \to \mathcal{L}(X, Z)$ such that

$$\lim_{h \to 0} \frac{1}{|h|} |F(x + h) - F(x) - G(x + h)h| = 0$$

for all $x \in U$.

If F is Newton differentiable then the Newton-algorithm applied to $F(x) = 0$ converges super-linearly.

For (P 2) and (P 3) the necessary optimality conditions cannot be expressed as operator equations with Newton differentiable operators. The complementary conditions associated to $y \leq \psi$ are formally given by

$$\lambda = max(0, \lambda + c(y - \psi)) \text{ for any } c > 0$$

. Regularizing this equation by

$$\lambda = \varepsilon max(0, \lambda + c(y - \psi)), \quad \varepsilon \in (0, 1)$$

provides a family of approximating equations each of which is Newton differentiable. We then study the path of solutions $\varepsilon \to (y_\varepsilon, \lambda_\varepsilon)$ for both (P 2) and (P 3) as $\varepsilon \to 1^-$ This path also has geometric properties which can be used advantageously in numerical realizations of path following techniques.

References

[IK 1] K. ITO and K. KUNISCH: Augmented Lagrangian Methods for Nonsmooth Convex Optimization in Hilbert Spaces, Nonlinear Analysis, Theory, Methods and Applications, 41(2000), 591–616.

[BIK] M. BERGOUNIOUX, K. ITO and K. KUNISCH: Primal-dual Strategy for Constrained Optimal Control Problems, SIAM J. Control and Optimization, 37(1999), 1176–1194.

[HIK] M. HINTERMÜLLER, K. ITO and K. KUNISCH: The primal–dual active set strategy as a semi–smooth Newton method, SIAM Journal on Optimization, 13(2002), 865-888.

[IK 2] K. ITO and K. KUNISCH: The primal-dual active set method for nonlinear optimal control problems with bilateral constraints, SIAM J. on Control and Optimization, 43(2004), 357-376.

[HK] M. HINTERMÜLLER and K. KUNISCH: Feasible and Non-Interior Path-Following in Constrained Minimization with Low Multiplier Regularity, SIAM J. Control and Optim., 45(2006), 1198-1221.

[IK 3] K. ITO and K. KUNISCH: Optimal Control of Obstacle Problems by H^1-Obstacles, Appl. Math. and Optim., to appear.

[VK] K. KUNISCH and B. VEXLER : Constrained Dirichlet Boundary Control in L^2 for a Class of Evolution Equations, to appear.

Optimal Control Challenges in Glass Production

René Pinnau

(joint work with Michael Herty, Mohammed Seaid)

To ensure the quality of the end product, many stages of the production process in glass industry can be – and have to be – influenced by control and optimization techniques. Since an appropriate modeling of the different stages has to include varying physical phenomena, this yields a whole hierarchy of PDE constrained optimization problems [3, 4]. Typically, they are involving heat diffusion and radiation coupled with PDEs for convection, visco–elasticity, or even MHD.

Here, we will give an overview on the state of the art in modeling, present first approaches to optimization of radiation dominant processes and show future perspectives. Especially, we discuss the radiative transfer problem which consists of a nonlocal integro–partial differential equation and the set–up for a corresponding tracking–type optimization problem. Further, we employ approximate models to describe radiative heat transfer, where an additional nonlinear heat equation has to be considered.

We emphasize that the overall challenge in optimal control of radiative heat transfer is the high dimensional discrete phase space of the discretized problem. Standard discretizations of the full set of equations often yield up to 10^{11} degrees of freedom.

The Model. The stationary radiative transfer equation can be written in general form [2] as

$$\omega \cdot \nabla I + (\sigma + \kappa) I = \frac{\sigma}{4\pi} \int_{S^2} I d\omega + \kappa B(T(t,x), \nu), \quad \forall\, \nu > \nu_0 \tag{1}$$

where $I(t, \nu, \omega, \mathbf{x})$ is the spectral intensity at time t, in position $\mathbf{x}$, within frequency ν and propagating along direction ω with speed c. In general, the unknown function $I(\cdot)$ depends on time $t \in \mathbb{R}^+$, frequency $\nu \in \mathbb{R}^+$, angle $\omega \in S^2$ and space $\mathbf{x} \in \mathbb{R}^3$ and has values in $\mathbb{R}$. In (1), S^2 denotes the unit sphere in $\mathbb{R}^3$, T is the temperature, $\kappa = \kappa(\nu, \mathbf{x})$ is the absorption coefficient, $\sigma = \sigma(\nu, \mathbf{x})$ is the scattering coefficient, ν_0 is the upper bound of opaque band of the optical spectrum where radiation is completely absorbed, and $B(T, \nu)$ is the spectral intensity of

the black-body radiation given by the Planck function

$$B(T,\nu) = \frac{2h\nu^3}{c_0^2}\left(e^{h\nu/kT}-1\right)^{-1},$$

where h, k and c_0 are Planck's constant, Boltzmann's constant and the speed of radiation propagation in vacuum, respectively. This equation is e.g. supplemented with Dirichlet boundary data

$$I(\omega,\mathbf{x}) = A, \qquad \mathbf{n}\cdot\omega < 0$$

for ingoing characteristics. In glass production the temperature is clearly also an unknown, such that one needs to couple the model with an additional nonlinear heat equation.

The Optimal Control Problem. For simplicity we consider here only an optimal control problem of tracking–type in radiative transfer, where the cost functional has the form

$$\mathcal{F}(R,Q) := \frac{\alpha_1}{2}\int_D \left(R-\bar{R}\right)^2 d\mathbf{x} + \frac{\alpha_2}{2}\int_D \left(Q-\bar{Q}\right)^2 d\mathbf{x}.$$

Here, $R(\mathbf{x}) := \int_{S^2} I(\omega,\mathbf{x})d\omega$ is the mean intensity and the radiative intensity I is given as the solution of (1). The control is the source term Q, which can be interpreted as a gain or loss of radiant energy deployed by external forces.

The general optimal control problem reads

$$\min_{R,Q} \mathcal{F}(R,Q) \text{ subject to (1).} \tag{2}$$

Remark 1. *Using the adjoint calculus one can derive the first–order optimality condition and prove the existence and uniqueness of an optimal control* [1].

The adjoint equation corresponding to (2) is given by

$$\begin{aligned} -\omega\cdot\nabla J(\omega,\mathbf{x}) + (\sigma+\kappa)J(\omega,\mathbf{x}) &= \frac{\sigma}{4\pi}\int_{S^2} J(\omega,\mathbf{x})d\omega + \alpha_1\left(R(\mathbf{x})-\bar{R}(\mathbf{x})\right), \\ J(\omega,\mathbf{x}) &= 0, \qquad \mathbf{n}\cdot\omega > 0, \end{aligned}$$

where $J(\omega,\mathbf{x})$ denotes the adjoint variable.

Numerical Results. We use this first–order derivative information in a gradient method for the numerical optimization [1] and present here numerical results for an optimal control problem in two space dimensions, where the radiant source is the control variable. The S_8-discrete ordinates set is used for the angle discretization in the radiative transfer equation and its associated adjoint problem. We use constant boundary data $A = 0$ and for the optimization we start with the initial guess $Q^0(\mathbf{x}) = 0$ for all $\mathbf{x} \in D$. Furthermore, the steplength in the gradient algorithm is chosen Armijo's rule. Note that already this two dimensional, grey problem involves $5\cdot 10^5$ degrees of freedom.

We set the desired source $\bar{Q}$ to be the sum of three Gaussian centered at $(x_1 = 1/4, y_1 = 3/4)$, $(x_2 = 1/4, y_2 = 1/4)$ and $(x_3 = 3/4, y_3 = 1/4)$, respectively, i.e.,

$$\bar{Q}(x,y) = \frac{1}{\sqrt{2}} \sum_{i=1}^{3} e^{-\frac{(x-\bar{x}_i)^2+(y-\bar{y}_i)^2}{2}}.$$

We solve the transport equation with source $\bar{Q}$ to obtain $\bar{R}$. Then we consider the source inversion problem,

$$\min \frac{\alpha_1}{2} \int_D \left(R - \bar{R}\right) dx + \frac{\alpha_2}{2} \int_D Q^2 dx.$$

In Figure 1 we present the given source and the reconstructed one. The location of the sources is well resolved while the strength of the sources is underestimated. Note, that we discarded all the information on the angular directions, i.e. we condensed the data used for the reconstruction by a factor 100. Despite of this fact the results are really encouraging.

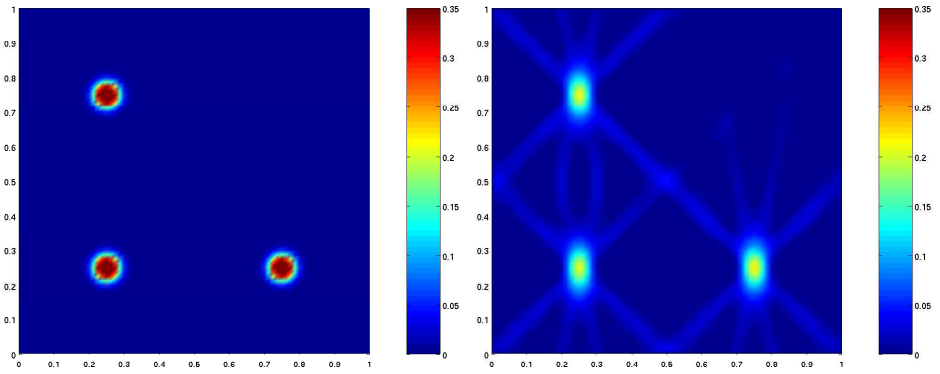

FIGURE 1. Desired control $\bar{Q}$ (left) and optimized control $Q(\mathbf{x})$ (right)

Conclusions. Present and future work is focused on the temperature coupling and the employment of asymptotic models, like the so–called SP_N equations [3, 4]. Here, first promising analytical and numerical results are available which underline the feasibility of this approach. Summarizing, one might say that the combination of appropriate models, fast solvers and model–based, well–suited optimization techniques allows for development of an optimization platform in radiative heat transfer, which can be used by industry. Nevertheless, several challenging problems, especially concerning multiphysics coupling, have to be addressed in the future.

REFERENCES

[1] M. Herty, R. Pinnau, M. Seaid. *Optimal Control in Radiative Transfer*. To appear in OMS, 2007.

[2] M. F. Modest, It Radiative Heat Transfer. McGraw-Hill, 1993.

[3] R. Pinnau, A. Schulze. *Newton's Method for Optimal Temperature-Tracking of Glass Cooling Processes*. To appear in IPSE, 2006.
[4] R. Pinnau and G. Thömmes. *Optimal boundary control of glass cooling processes*. M2AS, 120:1261, 2004.

Phase Field Modelling of Alloy Solidification

Björn Stinner
(joint work with Harald Garcke, Britta Nestler)

Mechanical properties as strength and also electrical properties of alloy workpieces are influenced by the arrangement of the solid grains on a scale of some micrometers. The microstructure is a result of the conditions imposed during the production process. In order to model the microstructure formation during the process of solidification we developed a general framework based on the phase field method [1]. It allows for arbitrary numbers M of phases and N of alloy components.

Let $e = c_0$ denote the internal energy and $c_1, \dots, c_N$ the concentrations of the alloy components. Balance equations for those conserved quantities read

$$\partial_t c_i = -\nabla \cdot J_i, \quad J_i = \sum_j L_{ij}(c,\phi)\nabla(-u_j(c,\phi)). \tag{1}$$

The diffusive fluxes J_i are assumed to be linear in the thermodynamic potentials which - essentially - are the temperature and the chemical potentials. Diffusivities enter the symmetric and positive semi-definite matrix of Onsager coefficients L_{ij} such that we can allow for cross diffusion effects.

Each component of the phase field variable $\phi = (\phi_1, \dots, \phi_M)$ describes the presence of a corresponding phase. They are subject to the system of Allen-Cahn type equations

$$\varepsilon\omega(\phi,\nabla\phi)\partial_t\phi_\alpha = \varepsilon(\nabla \cdot a_{,\nabla\phi_\alpha} - a_{,\phi_\alpha}) - \frac{1}{\varepsilon}w_{,\phi_\alpha} + s_{,\phi_\alpha}(c,\phi). \tag{2}$$

Here, the variable after a comma in the index denotes the partial derivative with respect to that variable. The function $\omega(\phi,\nabla\phi)$ is a kinetic coefficient, and the right hand side of the equation is the variational derivative of the entropy functional

$$S(c,\phi) = \int_\Omega \underbrace{s(c,\phi)}_{\text{bulk contribution}} - \underbrace{\left(\varepsilon a(\phi,\nabla\phi) + \frac{1}{\varepsilon}w(\phi)\right)}_{\text{surface contribution}}. \tag{3}$$

The coupling of the equations (1) and (2) is consistent with thermodynamics in the sense that an entropy inequality can be derived. As the diffuse interface thickness, scaling with ε, tends to zero a related sharp interface model is obtained. The domain is split into sub-domains corresponding to the phases with moving phase boundaries. In the phases there hold diffusion equations similar to (1). On the phase boundaries the thermodynamic potentials u_j are continuous, and

Rankine-Hugoniot conditions for the conserved quantities hold. The motion of the phase boundaries is furthermore governed by Gibbs-Thomson conditions.

To describe a certain alloy the general framework has to be calibrated. The bulk entropy density in (3) and the potentials u_j are given in terms of the free energy density $f(c, \phi)$. Certain forms of f lead to growth properties of the u_j in c that are analytically difficult to handle. Inverting the relation between u and c, i.e., writing the c_i as a function in (u, ϕ), the case $(c_i)_{,u} \to 0$ as $\|u\| \to \infty$ was considered.

Also the calibration with respect to surface energies leads to challenging problems [2]. Typically, surface energies $\gamma_{\alpha\beta}$ for the phase boundary between phases corresponding to the indexes α and β are known from experiments. The gradient potential $a(\phi, \nabla\phi)$ and the multi-well potential $w(\phi)$ in the surface contribution of the entropy (3) have to be adapted to recover the known energies in the sharp interface limit. Within this context it turns out to be favourable to avoid so-called third phase contributions, i.e., the presence of some phase in the interfacial layer between other phases.

The talk was closed with a short outlook on prescribing the microstructure characteristics that is to be achieved during the solidification process, which may be formulated as a control problem.

References

[1] H. Garcke, B. Nestler, B. Stinner, *A diffuse interface model for alloys with multiple components and phases*, SIAM J. Appl. Math. **64** (2004), 775–799.

[2] B. Stinner, *Surface energies in multi-phase systems with diffuse phase boundaries*, Int. Ser. Num. Math. **154** (2006), 413–423.

Phase Field Modelling of Multiphase Fluid Flows

Richard Welford

(joint work with David Kay, Vanessa Styles)

Phase field methods provide a convenient method of modeling multiphase fluid flow. They provide a natural method for dealing with the complex topological transitions that occur during the flow. The interface between the fluids is replaced by a thin transitional layer of width $O(\epsilon)$ where ϵ is a small parameter.

We consider the use of a Cahn-Hilliard-Navier-Stokes model for two-phase flow. If the fluids have the same density we have the following system of equations, known as Model H in the nomenclature of Hohenberg and Halperin [1, 2, 3]:

$$\partial_t c + \mathbf{u}\cdot\nabla c = \frac{1}{Pe}\nabla\cdot(b(c)\nabla w) \quad \text{in } \Omega_{\mathrm{T}} := \Omega\times[0,\mathrm{T}], \tag{1a}$$

$$w = \Phi'(c) - \epsilon^2\Delta c \quad \text{in } \Omega_{\mathrm{T}}, \tag{1b}$$

$$(\partial_t\mathbf{u} + \mathbf{u}\cdot\nabla\mathbf{u}) - \nu\Delta\mathbf{u} + \nabla p = Kw\nabla c \quad \text{in } \Omega_{\mathrm{T}}, \tag{1c}$$

$$\nabla\cdot\mathbf{u} = 0 \quad \text{in } \Omega_{\mathrm{T}}, \tag{1d}$$

$$\frac{\partial c}{\partial n} = 0, \qquad b(c)\frac{\partial w}{\partial n} = 0, \quad \mathbf{u} = \mathbf{h} \quad \text{on } \partial\Omega, \tag{1e}$$

$$c(\cdot,0) = c_0, \quad \mathbf{u}(\cdot,0) = \mathbf{u}_0, \quad \text{in } \Omega, \tag{1f}$$

where $c\in[-1,1]$ is the concentration of one of the fluid components, w is the chemical potential, $\mathbf{u}$ the mean velocity field, p the pressure, n the outward pointing unit normal of the domain, ϵ is a measure of the width of the interface, ν is the viscosity and Pe, K are constants. The function Φ is a double-well potential, $b(\cdot)$ is the mobility function. We have that:

$$\mathbf{u} = \frac{1+c}{2}\mathbf{u}_1 + \frac{1-c}{2}\mathbf{u}_2, \tag{2a}$$

$$\Phi(c) = \frac{1}{4}(1-c^2)^2, \tag{2b}$$

$$b(c) = (1-c^2)^2, \tag{2c}$$

where $\mathbf{u}_i,\ i=1,2$ is the velocity of the fluid component i.

This system is discretised using a finite element scheme. When discretizing care must be taken to ensure that essential features of the continuous system, such as mass conservation, are retained. A typical fully practical discretisation is:

$$\begin{aligned}
(\delta_t c_h^n,\eta)_h + (\mathbf{u}_h^{n-1}\cdot\nabla c_h^n,\eta) + Pe^{-1}(b(c_h^n)\nabla w_h^n,\nabla\eta) = 0 \qquad & \forall\,\eta\in S^h,\\
(w_h^n,\eta)_h = (\phi(c_h^n) - c_h^{n-1},\eta)_h + \epsilon^2(\nabla c_h^n,\nabla\eta) \qquad & \forall\,\eta\in S^h,\\
(\delta_t\mathbf{u}_h^n + \mathbf{u}_h^n\cdot\nabla\mathbf{u}_h^n,\boldsymbol{\chi}) + \nu(\nabla\mathbf{u}_h^n,\nabla\boldsymbol{\chi}) - (p_h^n,\nabla\cdot\boldsymbol{\chi}) = & K(w_h^n\nabla c_h^n,\boldsymbol{\chi})\\
& \forall\,\boldsymbol{\chi}\in(X_0^h)^2,\\
(\nabla\cdot\mathbf{u}_h^n,\xi) = 0 \qquad & \forall\,\xi\in S^h,
\end{aligned}$$

where

$$\delta_t v^n := \frac{v^n - v^{n-1}}{\tau}.$$

The finite element spaces are given by:
$S^h = \{v\in C(\overline{\Omega}) : v|_\kappa \text{ is linear } \forall\,\kappa\in T^h\}$,
$X^h = \{v\in C(\overline{\Omega}) : v|_\kappa \text{ is linear } \forall\,\kappa\in T^{h/2}\}$,
$X_0^h = \{v\in X^h : v = 0 \text{ on } \partial\Omega\}$,
where T^h and $T^{h/2}$ are finite element grids of size h and $h/2$ respectively. Using

this and similar discretisations convergence results and error estimates can be proved [5, 6].

The discrete problem is decoupled, leading to a solve for the Cahn-Hilliard system followed by a solve for the Navier-Stokes system at each timestep. The Cahn-Hilliard problem is solved using a nonlinear multigrid scheme [4, 5] that can be coupled to adaptive mesh techniques to yield an optimally efficient solver. The Navier-Stokes problem is solved using the F_p preconditioned GMRES scheme of Kay et al. [7].

If the fluids have different densities then model H no longer applies, and so we use the model of Boyer [8]. The solvers can be naturally extended to this case, and retain their optimality.

References

[1] P. C. Hohenberg and B. I. Halperin, *Theory of dynamic critical phenomena*,Rev. Mod. Phys., **49(3)** (1977), 435–479.

[2] John W. Cahn and John E. Hilliard, *Free Energy of a Nonuniform System. I. Interfacial Free Energy*, J. Chem. Phys., **28(2)** (1958) 258–267.

[3] C. M. Elliott, *The Cahn-Hilliard Model for the Kinetics of Phase Separation*, *in Mathematical Models for Phase Change Problems, J. F. Rodrigues (ed.), Birkhäuser Verlag* (1989) 35–73.

[4] David Kay and Richard Welford, *A Multigrid Finite Element Solver for the Cahn-Hilliard Equation*, *J. Comp. Phys.*, **212** (2006), 288–304.

[5] David Kay and Richard Welford, *Efficient Numerical Solution of Cahn-Hilliard-Navier-Stokes Fluids in 2D*, *to appear in SIAM J. Sci. Comp.* (2007).

[6] David Kay, Vanessa Styles and Richard Welford, *Finite element approximation of a Cahn-Hilliard-Navier-Stokes system*, *submitted to IFB.*

[7] David Kay,Daniel Loghin and Andrew Wathen, *Preconditioner for the Steady-State Navier-Stokes Equations*, *SIAM J. Sci. Comput.*, **24** (2002), 237–256.

[8] Franck Boyer, *A Theoretical and Numerical Model for the Study of Incompressible Mixture Flows*, *Comput. Fluids*, **31(1)** (2002), 41–68.

Control of the free boundary in a two-phase Stefan problem with flow driven by convection

Stefan Ziegenbalg

(joint work with Michael Hinze)

Introduction. The solidification process of a melt in a container is considered. The goal consists in controlling the evolution and the shape of the free boundary using the temperature on the container wall and/or near-wall Lorentz forces in order to achieve a prescribed shape of the solid-liquid interface.

Problem definition. The solidification process is modeled using the heat equation (1) in the solid phase Ω_s and in the liquid phase Ω_l. In the liquid phase additionally flow driven by convection and near-wall Lorentz forces (3), (4) is considered, where the convection term is modeled using the Boussinesq approximation. The phase transition is constituted by the Stefan condition (5) at the free

boundary Γ. The Robin-type boundary condition (6) models the heat transfer at the container wall $\partial\Omega$. Altogether one obtains the nonlinear system

$$
\begin{aligned}
&(1) && \partial_t u = \frac{k_s}{c_s \rho}\Delta u && \text{in } (0,T]\times\Omega_s,\\
&(2) && \partial_t u + \boldsymbol{v}\cdot\nabla u = \frac{k_l}{c_l\rho}\Delta u && \text{in } (0,T]\times\Omega_l,\\
&(3) && \nabla\cdot\boldsymbol{v} = 0 && \text{in } (0,T]\times\Omega_l,\\
&(4) && \partial_t \boldsymbol{v} + (\nabla\boldsymbol{v})\boldsymbol{v} - \frac{\varepsilon}{\rho}\Delta\boldsymbol{v} + \frac{1}{\rho}\nabla p = -\boldsymbol{g}\gamma(u-u_M) + \boldsymbol{A} && \text{in } (0,T]\times\Omega_l,\\
&(5) && V_\Gamma L = \frac{k_s}{\rho}\partial_{\boldsymbol{\mu}} u|_{\Omega_s} - \frac{k_l}{\rho}\partial_{\boldsymbol{\mu}} u|_{\Omega_l} =: -\Big[\frac{k_{s/l}}{\rho}\partial_{\boldsymbol{\mu}} u\Big]_\Gamma && \text{in } (0,T]\times\Gamma,\\
&(6) && \tfrac{k_{s/l}}{\alpha_{s/l}}\partial_{\boldsymbol{\nu}} u = u_b - u && \text{in } (0,T]\times\partial\Omega,\\
&(7) && u = u_M && \text{in } (0,T]\times\Gamma,
\end{aligned}
$$

Here, u denotes the temperature, u_M the melting temperature, $\boldsymbol{v}$ the velocity and p the pressure. The container wall temperature u_b and the Lorentz forces $\boldsymbol{A}$ are used as control variables. The free boundary is modeled as a graph $\Gamma(t) = \big\{(x,\ f(t,x))^T\big\}$. By $\overline{f}$ the desired evolution of the free boundary is denoted. The control goal mathematically is formulated as a pde-constrained optimization problem.

$$
\begin{aligned}
&J(f,u_b,\boldsymbol{A}) := \frac{1}{2T}\int_0^T\int_G \big(f(t,y)-\overline{f}(t,y)\big)^2 dy dt\\
&\qquad + \frac{\lambda_T}{2}\int_G \big(f(T,y)-\overline{f}(T,y)\big)^2 dy = \min_{f,u_b,\boldsymbol{A}}!\\
&\text{s.t. } (1)\text{ – }(7)\ .
\end{aligned}
\tag{P}
$$

The functional J models the objective in our minimization problem, namely the reduction of the error between the free boundary and the desired free boundary in the mean square sense. The parameter $\lambda_T > 0$ weighs the deviation of the free boundary from the desired free boundary at the final time $t = T$.

Solution of the minimization problem. The optimization problem (P) is solved using a adjoint approach, which allows to compute the gradient of the reduced functional $K(u_b,\boldsymbol{A}) = J\big(f(u_b,\boldsymbol{A}),u_b,\boldsymbol{A}\big)$ in a efficient way. The computational costs for one gradient computation consist in solving the forward system (1) – (7) with given $\boldsymbol{A}$, u_b and one backward-in-time adjoint system, which contains the state of the forward system as input data. Utilizing this an efficient gradient method is developed.

Results. We examine an Aluminium melt in a rotational symmetric cylinder. The desired free boundary is a moving plane. The figures show the state at different time instances, for the uncontrolled problem (left), and for the controlled problem (right) after a suitable stopping criterion is met. The black line depicts the free boundary, the white and grey stripes show the temperature and the arrows depict

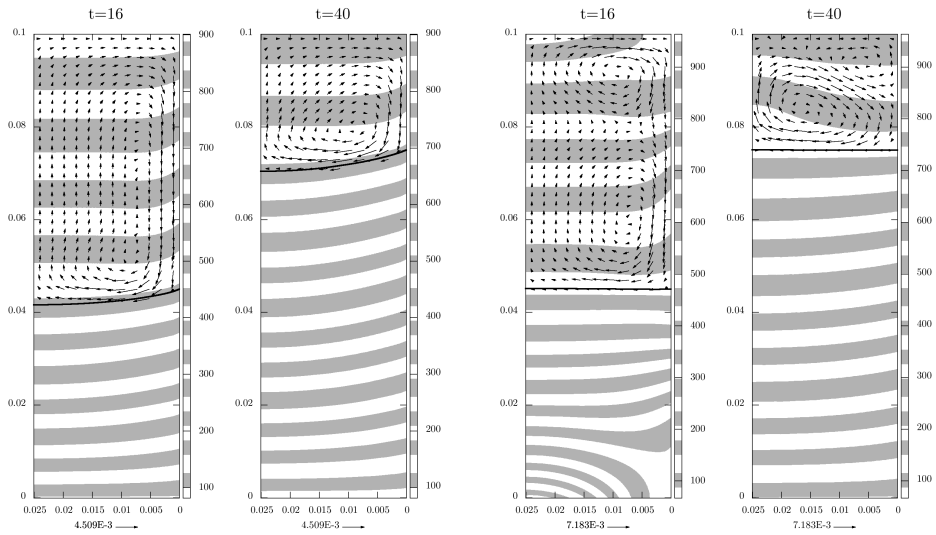

without control with control

the velocity. One clearly sees that tracking of the desired free boundary, a flat graph, works very well. Details are given in [1, 2]. For a related approach we refer to [3].

References

[1] M. Hinze, S. Ziegenbalg. *Optimal control of the free boundary in a two-phase Stefan problem*, J. Comput. Phys. (2006), doi:10.1016/j.jcp.2006.09.030, see also Preprint SFB609-2-2005, http://www.tu-dresden.de/sfb609/Preprints/2005/SFB609-Preprint-02-2005.pdf.

[2] M. Hinze, S. Ziegenbalg. *Optimal control of the free boundary in a two-phase Stefan problem with flow driven by convection*, Preprint SFB609-2-2006, http://www.tu-dresden.de/sfb609/Preprints/2006/SFB609-Preprint-02-2006.pdf

[3] N. Zabaras, T. Hung Nguyen. *Control of the freezing interface morphology in solidification processes in the presence of natural convection* International Journal for Numerical Methods in Engineering **38** (1995), 1555–1578.

Reporter: Charles M. Elliott, Michael Hinze, and Vanessa Styles

Participants

Prof. Dr. Eberhard Bänsch
Lehrstuhl f. Angew. Mathematik III
Universität Erlangen
Haberstr. 2
91058 Erlangen

Prof. Dr. Klaus Deckelnick
Institut für Analysis u. Numerik
Otto-von-Guericke-Universität
Magdeburg
Universitätsplatz 2
39106 Magdeburg

Prof. Dr. Gerhard Dziuk
Abteilung f. Angewandte Mathematik
Universität Freiburg
Eckerstr. 1
79104 Freiburg

Prof. Dr. Charles M. Elliott
Department of Mathematics
University of Sussex
Falmer
GB-Brighton, East Sussex BN1 9RF

Prof. Dr. Heike Emmerich
Institut für Gesteinshüttenkunde
RWTH Aachen
Maurerstr. 5
52064 Aachen

Dr. Harald Garcke
NWF-I Mathematik
Universität Regensburg
93040 Regensburg

Dr. Roland Griesse
Johann Radon Institute
Austrian Academy of Sciences
Altenberger Straße 69
A-4040 Linz

Prof. Dr. Michael Hintermüller
Institut für Mathematik
Karl-Franzens-Universität Graz
Heinrichstr. 36
A-8010 Graz

Prof. Dr. Michael Hinze
Department Mathematik
Universität Hamburg
Bundesstr. 55
20146 Hamburg

Prof. Dr. Karl Kunisch
Institut für Mathematik und
wissenschaftliches Rechnen
Karl-Franzens-Universität Graz
Heinrichstr. 36
A-8010 Graz

Prof. Dr. Rene Pinnau
Fachbereich Mathematik
T.U. Kaiserslautern
Erwin-Schrödinger-Straße
67653 Kaiserslautern

Prof. Dr. Kunibert G. Siebert
Institut für Mathematik der
Universität Augsburg
Universitätsstr. 14
86159 Augsburg

Björn Stinner
Department of Mathematics
University of Sussex
Falmer
GB-Brighton, East Sussex BN1 9RF

Dr. Vanessa Styles
Department of Mathematics
University of Sussex
Falmer
GB-Brighton, East Sussex BN1 9RF

Priv.Doz.Dr. Axel Voigt
Crystal Growth Group
Research Center CAESAR
Ludwig-Erhard-Allee 2
53175 Bonn

Stefan Ziegenbalg
Institut für Numerische Mathematik
TU Dresden
Zellescherweg 12-14
01062 Dresden

Dr. Richard Welford
Department of Mathematics
University of Sussex
Falmer
GB-Brighton, East Sussex BN1 9RF